國 立 成 功 大 學

太空與電漿科學研究所

碩士論文

National Cheng Kung University

Institute of Space and Plasma Sciences

Master Thesis

小型脈衝功率之除鏽裝置

Rust Remover Using Small Pulsed-Power System

研究生：黃梅鳳

指導老師：張博宇博士

中華民國一百零六年七月

國立成功大學

碩士論文

小型脈衝功率之除鏽裝置

Rust remover using small pulsed-power system

研究生：黃梅鳳

本論文業經審查及口試合格特此證明

論文考試委員：

陳秋榮

陳孝輝

張博宇

指導教授：張博宇

系(所)主管：陳炤彰

中　華　民　國　106　年　7　月　20　日

摘要

現今工業快速發展當中，鐵製品已經大量的存在我們生活當中。然而，首當其衝的問題是，鐵製品容易生鏽。因此，此篇論文研究主題，希望透過建立一個小型的脈衝功率系統來達成除鏽的目的。我們利用集膚效應(skin effect)的原理，將一個短脈衝、高功率的電流傳遞到有鏽的金屬表面，藉此將能量釋放到金屬表面，將鏽從固態加熱至汽態蒸發，完成除鏽的功能。我們的小型脈衝功率系統內部包含兩個 40 nF 的電容串聯，將電容分別充到 ±8 kV 儲存 2.56 J 的能量。為了製作小型的脈衝功率系統，我們建製了一個耐壓達 16 kV 的間隙開關(spark gap switch)，及一個使用汽車點火線圈製作而成的脈衝觸發產生器，提供上升時間(rise time，定義為四分之一週期)為 55.0±0.4 μs、輸出電壓為 -18 kV 觸發脈衝訊號。此小型脈衝功率系統最後可輸出一個上升時間為 5.2 ± 0.2 μs，最高輸出電流為 15.9 ± 0.6 kA 的脈衝電流，相對應的系統電感值、電阻值及鐵表面的集膚深度(skin depth)分別為 212 ± 85 nH、1.00 ± 0.04 Ω、0.4μm，電流的角頻率為$(4.9 \pm 0.1) \times 10^{6}\ sec^{-1}$。系統的總放電時間為 11 μs，估算出系統的總輸出平均功率為 230 kW。我們預期每一次的放電(discharge)將可以除去面積約 1.8 cm x 1.8 cm 的鏽。我們針對相同的鐵鏽放電了至少 2500 次，然而，效果並不如預期，並沒有觀察到顯著的除鏽效果。推測原因是因為能量不止只有釋放到鐵鏽的表面，還有釋放到了電流流經系統放電迴路中所有的金屬表面上。但是藉由此結果可以知道，未來我們實驗室將要建立的脈衝功率系統，其中的金屬導線不會因為大電流的放電而被侵蝕。

關鍵字: 脈衝功率系統; 觸發脈衝產生器; 間隙開關

Abstracts

A rust remover was built using a small pulsed-power system. It is very important since there are a lot of iron products that exist in our daily life. A common problem of all iron tools is that they rust. The rust remover we built is to remove rust using the skin effect of a short pulse current propagating through rusted metal surface. To provide a high current, a small pulsed-power system using two 40 nF capacitors connected in series charged to ~ ± 8 kV storing 2.56 J of total energy was built. A controlled spark gap that can hold up to 16kV voltage was built. To trigger the spark gap, a high voltage trigger pulse generator providing a -18 kV trigger pulse with 55.0 ± 0.4 μs rise time was built by using an ignition coil for cars. In this small pulsed-power system, the rise time of the current (quarter period), the calculated skin depth of iron, and the peak current are 5.2 ± 0.2 μs, 0.4 um and 15.9 ± 0.6 kA, respectively, with an fitted inductance of 212 ± 85 nH and fitted resistance of 1.00± 0.04 Ω. The oscillation frequency is (4.9 ± 0.1) x 10^6 sec^{-1}. The averaged power of our pulsed-power system is about 230 kW before the output current is fully damped in ~ 11 μs. Rust on an iron surface, ~1.8 cm long and ~1.8 cm wide, was expected to be removed in each discharge. More than 2500 shots on the same rusted object were conducted. Unfortunately, the result didn't meet our expectation and no significant amount of rust was removed. The most possible reason is that the energy was released not only on the rusted surface but also on any (metal) surface along the current path. However, it shows that we don't need to worry about the erosion on the cables in a pulsed-power system which will be built as the long term goal in our lab.

Keywords: Pulsed-power system; Marx generator; Trigger pulse generator; Spark gap switch

Contents

Table

Figure

Chapter 1 INTRODUCTION

Nowadays, there are a lot of iron products that exist in our daily life. A common problem of all iron tools is that they rust. The rust remover we built is to remove rust using the skin effect of a short pulse current flowing through rusted metal surface. The principle of skin effect is shown in Section 1.1. The different kinds of rust removers are shown in Section 1.2. The design of out rust remover using a pulsed-power system is shown in Section 1.3. In Chapter 2, Puled power system and some key elements of the system are introduced. In Chapter 3 shows the details of how the pulsed-power system is implemented. In Chapter 4, the test result of the rust remover will be discussed. A summary is given in Chapter 5.

1.1 The principle of the skin effect

The skin effect is the attenuation of an alternating electric current (AC) penetrating into a conductor. The current density is the largest near the surface of the conductor and decreases as it goes deeper into the conductor. In other words, the electric current flows mainly in the "skin" of the conductor, between the solid line and dash line which are shown in Figure 1.1, called the skin depth.

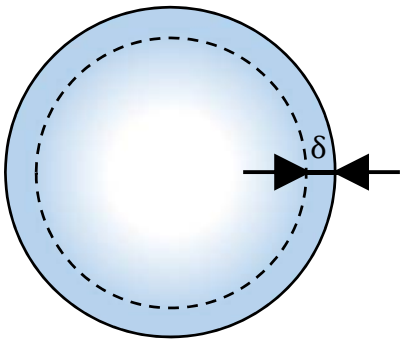

Figure 1.1 The skin depth is between dash the line and the solid line. The current flows either into or out of the paper.

In high frequency, the skin depth is small. It reduces the effective cross-section of the conductor so that the resistance of the conductor increases. The general formula for the skin depth [10] is

$$\delta = \sqrt{\frac{2 \times \rho}{\mu \times 2\pi f}} \tag{1.1}$$

where ρ, μ and f are the resistivity of the conductor, the permeability and the frequency of the current, respectively. The parameters of iron, which is considered in this thesis, are ρ_{Fe} = 97.1 (Ω· nm) and μ_{Fe}= 0.25（H· m^{-1}）.

1.2 Different kinds of rust remover

There are several kinds of tools that can be used in removing rust. The easiest way is to scratch off the rust directly. One alternative method is using LASER to remove rust. The principle of using LASER is to output high energy and focus it on a small area in a very short period of time. The reflectivity of a rustic surface is much less than a non-rustic surface. Based on different reflectivity between the rust and the conductor shown in Figure 1.2, the rust will absorb more energy and quickly be heated and vaporized.

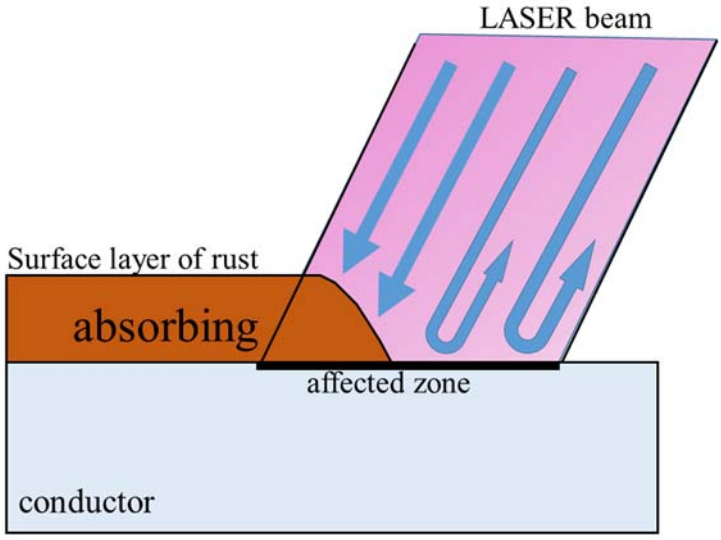

Figure 1.2 Illustration of LASER beam activity on the surface of the conductor

The chemical method can also be used to remove rust. The chemical method is uses acidic solvent. Because the major element of the rusted iron is Fe_2O_3, it can be dissolved in acidic solvent and removed.

1.3 A rust remover using the pulsed-power system

In this thesis, we study the method of using a small puled-power system to output electrical energy within a short pulse and heat the rust until it is vaporized. We design the pulsed-power system consisting of two 40 nF capacitors charged to ±10 kV and one switch connected in series storing 4J of total energy when it is fully charged. The design of the rust remover including the pulsed-power system is illustrated in Figure 1.3. We estimated that the rust on an iron surface, ~ 1.8 cm long and ~ 1.8 cm wide, can be removed in each discharge when the high current flows through the surface. The details are given in the following.

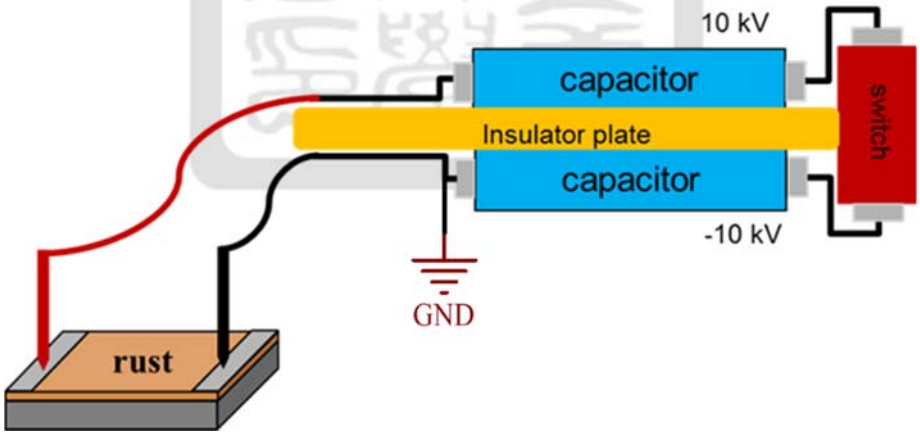

Figure 1.3 There are two capacitors and one switch connected in series. The proposed pulsed-power system will use two 40 nF capacitors charged to ±10 kV and total store energy will be 4 J.

When the system discharges, it provides a large current in a short period of time. The frequency of the pulsed current is very high. The current only propagates through and cleans

the rusted metal surface due to the skin effect. We assume that the total inductance of our system is 100 nH, and the peak current is $I \approx \frac{V}{\sqrt{L/C}} = 9kA$. The angular frequency of the current output, $\omega = 2\pi f = \frac{1}{\sqrt{LC}} \sim 20M\ sec^{-1}$. Thus, the rise time $T \approx \frac{1}{4}\frac{2\pi}{\omega}$ = 70 ns and the skin depth of iron for the pulsed current is

$$\delta_{Fe} = \sqrt{\frac{2 \times \rho_{Fe}}{\mu_{Fe} \times 2\pi f}} = 0.19um \tag{1.2}$$

where ρ_{Fe}= 97.1 (Ω· nm) and μ_{Fe} = 0.25（H· m^{-1}）.

We estimated how much rust can be removed in the following. The volume of the rust that will be removed in each discharge is illustrated in Figure 1.4 where δ_{Fe} is the skin depth, W is the width and L is the length between electrodes.

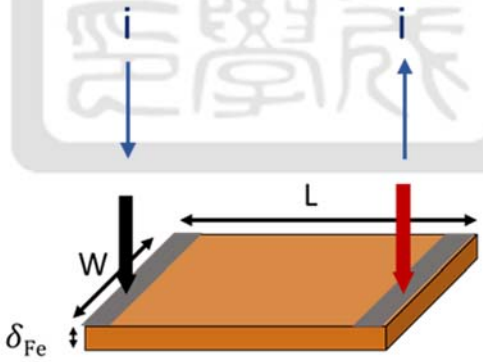

Figure 1.4 Illustration of rust volume can to be removed.

When the current prorogates through the volume, the volume is heated due to the Ohmic heating. If the energy is enough, the rusted iron can be melt and vaporized. The progress of phase changes of the iron is illustrated in Figure 1.5. The 1st and the 3rd regions are the solid

and liquid states while the 2nd and the 4th regions represent the process of melting and vaporizing.

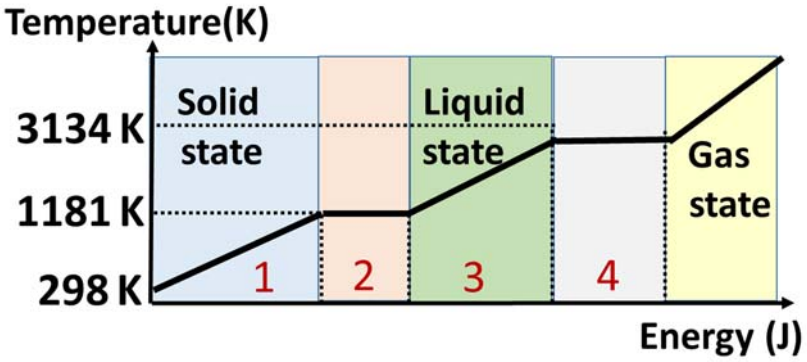

Figure 1.5 Process of phase changes progress of rust

In both solid and liquid state (region 1 and 3), the required heat energy is

$$H(J)=M \times S \times \Delta t \tag{1.3}$$

where M is the mass of the rust, S is the specific heat and Δt is the temperature difference of the rust. Therefore, the required heating energy at the melting and boiling temperature are given by $H_1 = M \times 646 \times (1811-298)$ and $H_3 = M \times 824 \times (3134-1811)$, respectively, where 1,811 and 3,134 are the melting point and the boiling point in Kelven, 646 J/kg-K is the averaged specific heat of iron in solid and 824 J/kg-K is the averaged specific heat of iron in liquid phase. When the phase is changing, the latent heat is $H_2 = M \times (250 \times 10^3)$ and $H_4 = M \times (6120 \times 10^3)$ where 250×10^3 and $6{,}120 \times 10^3$ are enthalpy of fusion and vaporization. The mass of the removed region is

$$\begin{aligned} M = dV &= d\,(W \times L \times \delta_{Fe}) \\ &= 7874\,(W \times L \times 0.19 \times 10^{-6}) \\ &= Z \times 1.5 \times 10^{-3}\ (kg) \end{aligned} \tag{1.4}$$

where $d = 7{,}874\ kg/m^3$ is the iron mass density and $Z \equiv W \times L\ m^2$.

The calculated heat energy of each part is listed as following.

(1) $H_1 = (Z \times 1.5 \times 10^{-3}) \times 646 \times (1811\text{-}298) = 1466Z$.

(2) $H_2 = (Z \times 1.5 \times 10^{-3}) \times (250 \times 10^3) = 375Z$.

(3) $H_3 = (Z \times 1.5 \times 10^{-3}) \times 824 \times (3134\text{-}1811) = 1635Z$.

(4) $H_4 = (Z \times 1.5 \times 10^{-3}) \times (6120 \times 10^3) = 9180Z$.

$H_{total} \approx 1466Z + 370Z + 1635Z + 9200Z = 12{,}671Z$.

If all the stored energy, 4J, in the pulsed-power system is released to the rust, i.e., it equals the thermal energy required to vaporize the rust, the area of the removed region in each discharge is

$$\begin{aligned} 4(J) &= 12671Z \\ Z \approx W \times L &\approx 0.018m \times 0.018m \\ &\approx 1.8\ cm \times 1.8\ cm \end{aligned} \tag{1.5}$$

To remove more surface or thicker rust, the application of many discharge will be required. After estimating the required energy, for removing the rust we can start to build our pulsed power system. With the above estimate, it seems feasible to remove the rust using a pulsed-power system.

Chapter 2 PULSED-POWER SYSTEMS

A pulsed-power system stores energy first and releases electrical energy into a load in a single short pulse to achieve high power output. In a general conductive pulsed-power system, it consists of an energy bank, e.g., capacitors, a closed switch, and a trigger pulse generator. A trigger pulse is used to activate the switch. In this Chapter, the basic knowledge of a RLC circuit is given in Section 2.1. In Section 2.2, different methods of building pulsed-power systems are introduced. In Section 2.3, one of the key components, closed switch, is introduced.

2.1 RLC circuit

The basic unit of any pulsed-power systems is a simple RLC circuits. A RLC circuit is an electrical circuit consisting of a resistor (R), an inductor (L), and a capacitor (C), connected in series or in parallel. Figure 2.1 is the RLC circuit connected in series. The energy is stored in the capacitor first and released to the inductor and the resistor. The process of releasing energy to the inductor is called discharge. Our rust remover system circuit is based on this simple RLC circuit.

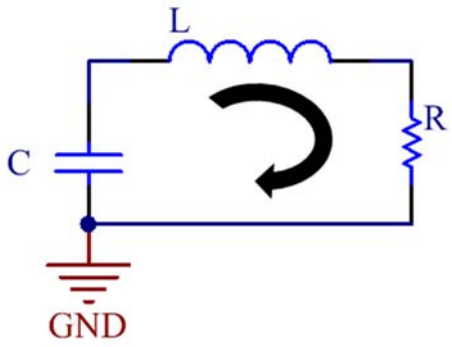

Figure 2.1 The RLC circuit connected in series.

The characteristic of the discharge current can be calculated analytically by the circuit equation:

$$V - IR - L\frac{dI}{dt} = 0\,, \tag{2.1}$$

with current

$$\mathrm{I} = \frac{dQ}{dt} = -C\frac{dV}{dt}\,, \tag{2.2}$$

$$\mathrm{V} + \mathrm{RC}\frac{dV}{dt} + LC\frac{d^2V}{dt^2} = 0\,, \tag{2.3}$$

$$\frac{d^2V}{dt^2} + \frac{R}{L}\frac{dV}{dt} + \frac{1}{LC}V = 0\,. \tag{2.4}$$

Initial conditions of the analytical solution is that the voltage of the capacitor at t = 0 is V (t = 0) = V_0, I (t = 0) = 0.

Let $V = V_0 e^{Dt}$ and substitute it into equation (2.4):

$$V = V_0 e^{Dt} = V_0 e^{-\frac{R}{2L}t}\left[e^{\sqrt{\left(\frac{R}{2L}\right)^2 - \frac{1}{LC}}t} + e^{-\sqrt{\left(\frac{R}{2L}\right)^2 - \frac{1}{LC}}t}\right]. \tag{2.5}$$

The current can be obtained via $\mathrm{I} = -\mathrm{C}\frac{dV}{dt}$. The details of the derivation are shown in Appendix. The solution can be caretorized in three cases: critical damped, under damped and over damped.

1. Under damped condition where $\left(\frac{R}{2L}\right)^2 - \frac{1}{LC} < 0$:

$$\mathrm{I(t)} = \frac{V_0}{\sqrt{\frac{L}{C} - \left(\frac{R}{2}\right)^2}} e^{-\frac{R}{2L}t} \sin\left[\sqrt{\frac{1}{LC} - \left(\frac{R}{2L}\right)^2}\, t\right]. \tag{2.6}$$

2. Critical damped condition where $\left(\frac{R}{2L}\right)^2 - \frac{1}{LC} = 0$:

$$\mathrm{I(t)} = \frac{V_0}{L} t e^{-\frac{R}{2L}t}\,. \tag{2.7}$$

3. Over damped condition where $\left(\frac{R}{2L}\right)^2 - \frac{1}{LC} > 0$:

$$\mathrm{I(t)} = \frac{V_0}{\sqrt{\left(\frac{R}{2}\right)^2 - \frac{L}{C}}} e^{-\frac{R}{2L}t} \sinh\left(\sqrt{\frac{1}{LC} - \left(\frac{R}{2L}\right)^2}\, t\right). \tag{2.8}$$

These three cases are shown in Figure 2.2. The red line is for the under damped case, the blue line is for the critical damped case and the black line is for the over damped case.

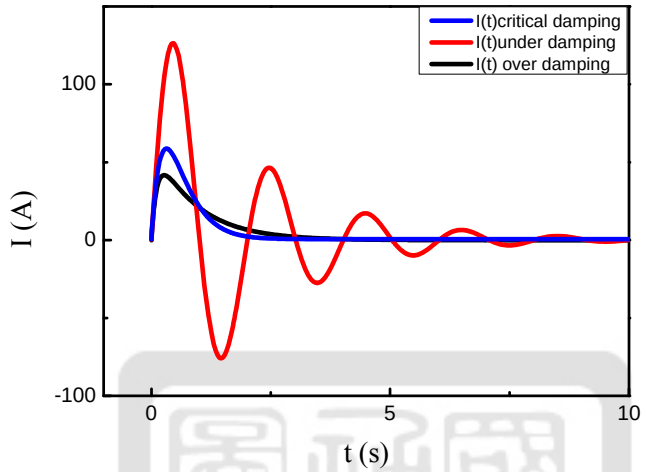

Figure 2.2 The current on the three cases: critical damping, under damping and over damping. Shown in red, blue, and black line.

2.2 Different methods of building a pulsed-power system

In a pulsed-power system, energy needs to be stored in an energy bank either capacitively or inductively. Inductive storage is effective but open switches are needed. Open switches are difficult to build. On the contrary, capacitive storages with closed switches are easier to be implemented. Therefore, we are using the capacitive storage. Two kinds of conductive pulsed-power systems, Marx generators and Linear transformer drives, will be introduced in section 2.2.1 and section 2.2.2, respectively.

2.2.1 Marx generators

Marx generator is used to provide high voltage output using relatively low voltage input. It is a unique circuit for voltage multiplication, as showing in Figure 2.3 [2][7]. High-voltage

pulse capacitors are mostly built for operating voltage below 100 kV. The main reason is that transformers for high-power charging supply units become prohibitively large when the output voltage is larger than 100 kV. A Marx generator is a easy way to provide high voltage output by using low voltage capacitors and power supplies.

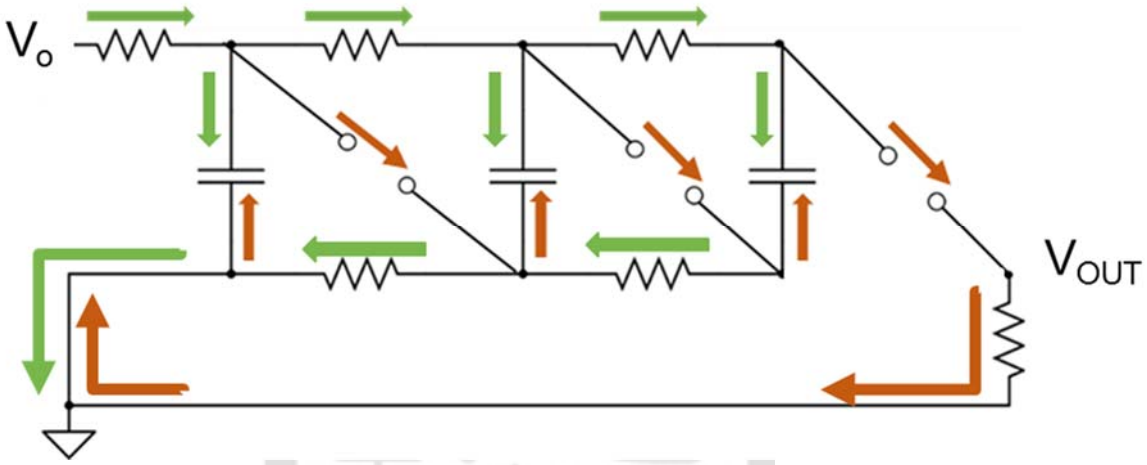

Figure 2.3 Three-stage Marx generator circuit.

Figure 2.3 shows a three-stage Marx generator as an example. During the charging phase, capacitors are connected in parallel. Current flow follows green arrows and voltages across capacitors increase when the most left switch is switched on, and the current can flow through it. During the discharge phase, current follows orange arrows. The fundamental principle of this kind of generator is to charge several capacitors connected in parallel and to switch them into series connection during discharge. The output voltage is given by the charging voltage multiplied by the number of capacitors and high voltage output is achieved.

2.2.2 Linear transformation drivers

Linear transformer drivers (LTDs) are a rapidly developing pulsed-power technology that are capable of delivering high-power, high-current, 100–300 ns output pulses in a compact configuration [3-6]. LTDs consist of several capacitors, switches and magnetic

cores. The basic units of LTDs are called bricks. Each brick comprised internally of two capacitors and a gas switch connect in series. The cross-section structure of a brick is shown in Figure 2.4[3]. When the trigger pulses are delivered into switches and induce breakdown in switches, capacitors will release the energy and the currents flow in the path of the solid red line. The leakage currents along the dashed red line is very little since the inductance of the path along the dashed line with the magnetic core is much larger than the one along solid line.

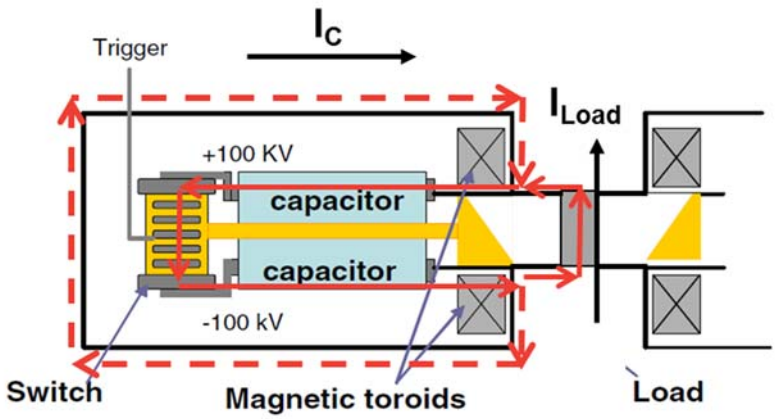

Figure 2.4 The cross-section of a brick in the LTDs. Each brick has two capacitor and a switch connected in series. Capacitors in either ends of the switch will be charged to ±100 kV. The switch must hold 200 kV. Trigger pin is used to deliver a trigger pulse to induce switch breakdown.

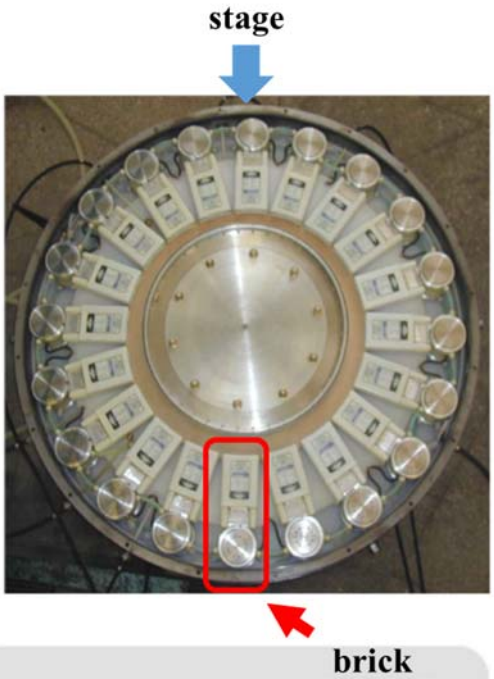

Figure 2.5 The structure of the LTDs. There are 20 bricks inside the LTDs.

Figure 2.6 A lot of stages connected in series.

To provide high current output, many bricks can be connected in parallel which is called a stage and shown in Figure 2.5[5]. To connect many stages in series, high voltage output can be generated as shown in Figure 2.6[14]. In order to output a short pulse, i.e., a high-peak-power pulse, all switches need to be activated at the same time. The controllable switches

has a stringent demand for the time of breakdown. Nevertheless, a high-power, high-current, short pulse can be delivered in this compact configuration.

A linear transformer driver is a compact puled-power system that can generate short pulses. However, the challenge is that all the switches need to breakdown simultaneously. It is difficult to implement and will not be used in our laboratory.

2.3 Switches

Switches are one of the most important elements in pulsed-power systems. High-power switches are the connecting elements between the storage device and the load[2]. Gas switches are commonly used in high-power pulse generators. They are easily built and they can handle large current. Different switches operate in very different pressure regions. The range of gas pressure and operating voltage for some of the most important switches are shown in Figure 2.7[2].

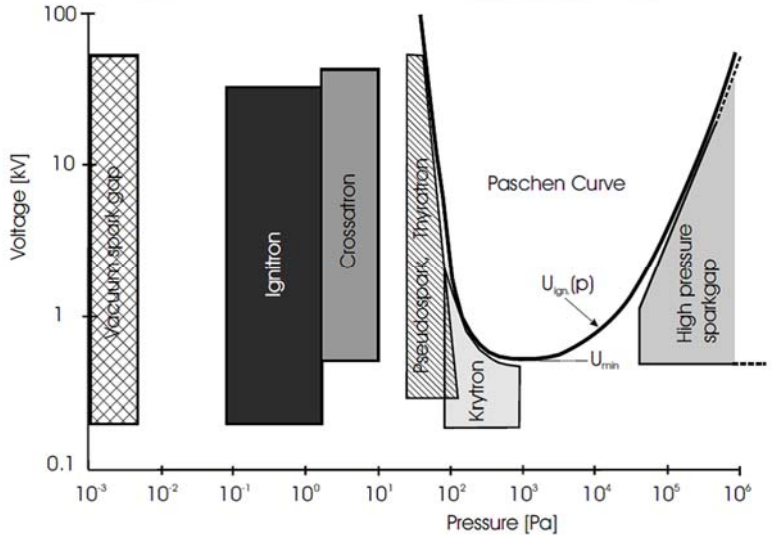

Figure 2.7 The range of gas pressure and operating voltage for some of the most important types of gas-filled switches. In addition, Paschen curve for air is shown for a fixed gap width of 3 mm.

For all switches systems, the operation can be divided into four phases shown in Figure 2.8:

(1) Trigger phase: A trigger pulse is delivered to the switch at the beginning of this phase. A trigger discharge occurs leading to a small voltage drop in the switch.

(2) Transition phase: It is also called commutation phase where the switch impedance transistor changes from a high to a low value. The voltage across the switch starts to drop while the current increases dramatically.

(3) Stationary phase: in this phase, the voltage drop is minimum and the current is maximum.

(4) Recovery phase: when the current release is finished the voltage will increase again.

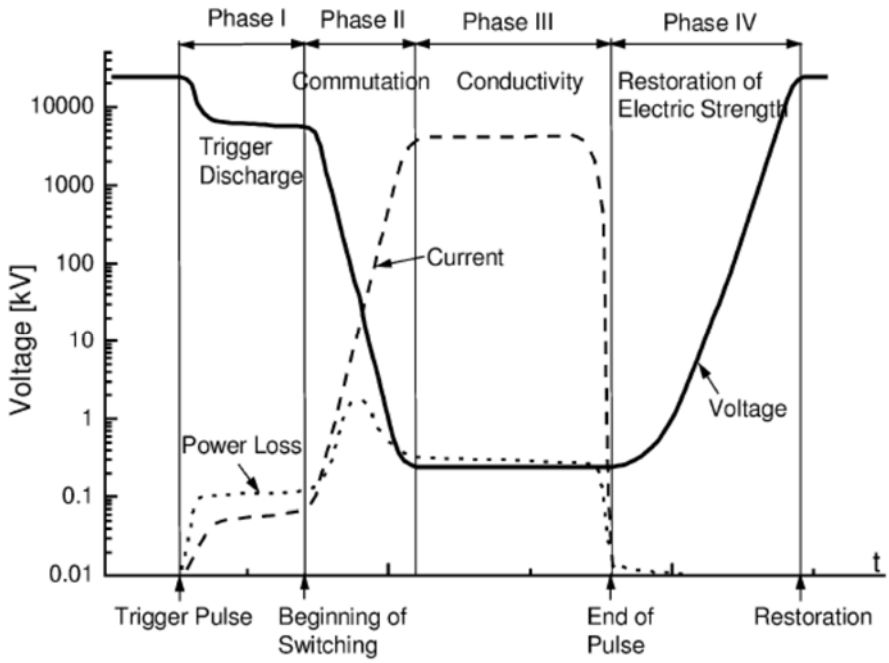

Figure 2.8 Evolution of voltage, current and power loss in a gas-filled switching system.

Considerable energy consumption occurs only during the commutation phase where the voltage drops and the current increases dramatically.

2.3.1 Paschen curve and breakdown voltage

The dielectric strength of a gas is determined by the magnitude of its atomic and molecular reaction cross-section for electron collisions. Other factors affecting the electric strength are the sample geometry, the pressure, the temperature, and the electric material. Dielectric breakdown is a statistical phenomenon. One cannot predict with certainty the time of breakdown, one may only calculate the probability of breakdown under given conditions of fields and geometries. At the microscopic level, breakdown requires the presence of sufficiently energetic charged particles. In most cases, electrons dominate the breakdown process since their mobility is much larger than that of ions. Figure 2.9 is the relationship between the breakdown voltage in air and the gap distance times pressure (pd). It is called Paschen curve. It shows that at high pd, the breakdown voltage increases as pd increases. It is because the collision rate increases, i.e., mean free path decreases, as the pressure goes up. The electron energy gains from the electric field decreases in each collision with atoms. Even though the collision rate increases, the effective collision between electrons and atom is low. It needs to increase the applied voltage to increase the number of effective collisions. However, at low pd regime, the breakdown voltage also increases when pd decreases. In this regime, the mean free path of electrons is long and they can be accelerated to high velocity. But the collision rate becomes so low such that almost no collision happens. The curve can be used to design a spark gap. If one can operate a switch from the region below the curve to the region above the curve, the switch can be activated.

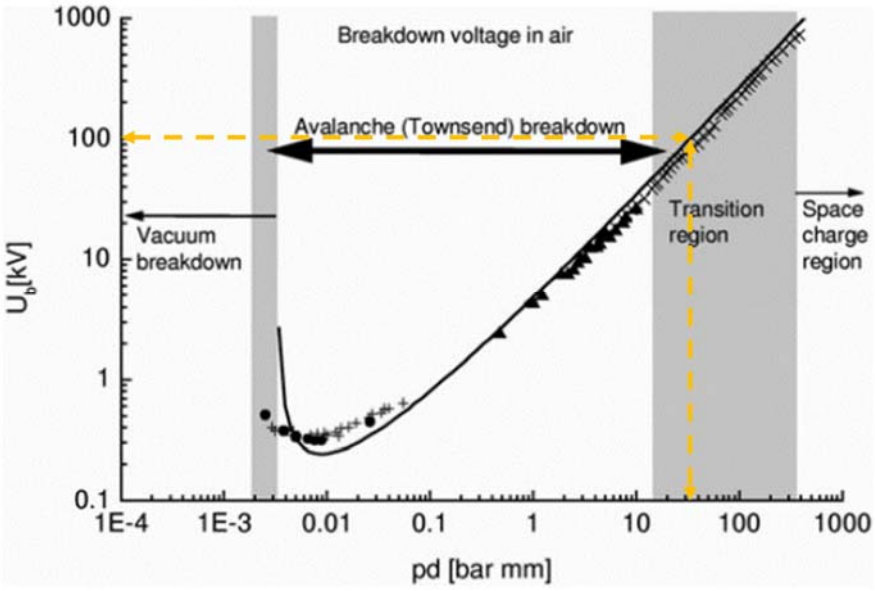

Figure 2.9 Measured and calculated Paschen curve for atmospheric air.

2.3.2 Gas-filled Spark gaps

A spark gap can be breakdown not only because the operation voltage exceeds its breakdown voltage but also due to certain events, such as UV radiation, plasma diffusion, etc, inside the spark gap. We will use the method of changing the electric field strength to control the activation of our switch. In Figure 2.10, it is a spark gap switch with trigger pin. There are two blue electrodes with a gap distance (d_1) between them. Purple electrode is a trigger pin and located at a distance (d_2) with blue electrodes ($d_1=2d_2$ in our design given later). For example, when 10kV is applied to the left blue electrode, -10kV to the right electrode and the trigger pin is grounded (0kV), the distance d_1 and d_2 need to hold the voltage differences so that the spark gap switch does not breakdown. When a -10kV trigger pulse is delivered to the trigger pin, the voltage between the left blue electrode and the trigger pin is 20kV. The d_2 is designed such that it cannot hold the voltage, a breakdown occurs on the left half. After left side breakdowns, the voltage of the trigger pin becomes 10kV leading to the breakdown in the right half. There is an example of gas-filled switchs designed by

Kinetech LLC [5] in Figure 2.11.

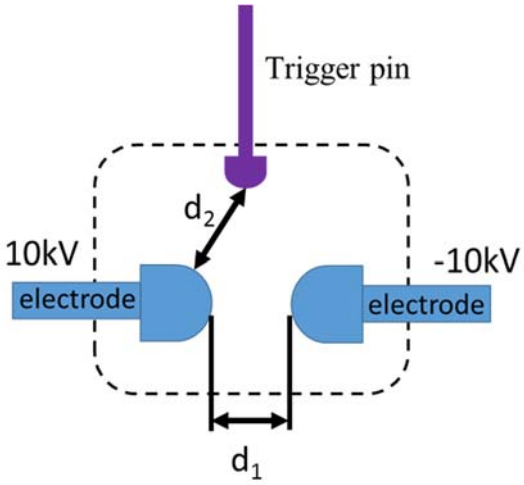

Figure 2.10 A spark gap switch with trigger pin.

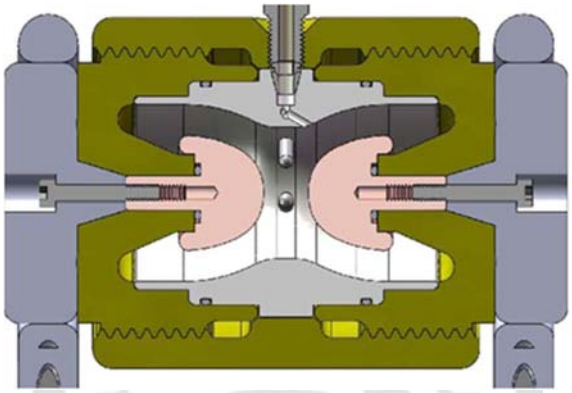

Figure 2.11 Cross-section of the gas-filled spark gap designed by Kinetech LLC.

This switch has two hemispherical electrodes. The distance between two electrodes can be adjusted by screws. In stead of using only one trigger pin, four trigger pins are used. Therefore, erosion of trigger pins reduce and lifetime of this switch can be extended. The reason is that the breakdown across one electrode to one of trigger pins occurs first. A sequential breakdown may occur between a different trigger pin to the other electrode. In Figure 2.12(a), the contour plots of amplitude of electric fields in the Kinetech switch with 200 kV between electrodes are shown. The trigger pin is grounded (0 kV) and there are ± 100 kV applied to the electrodes. At this moment, the gap is holding the voltage.

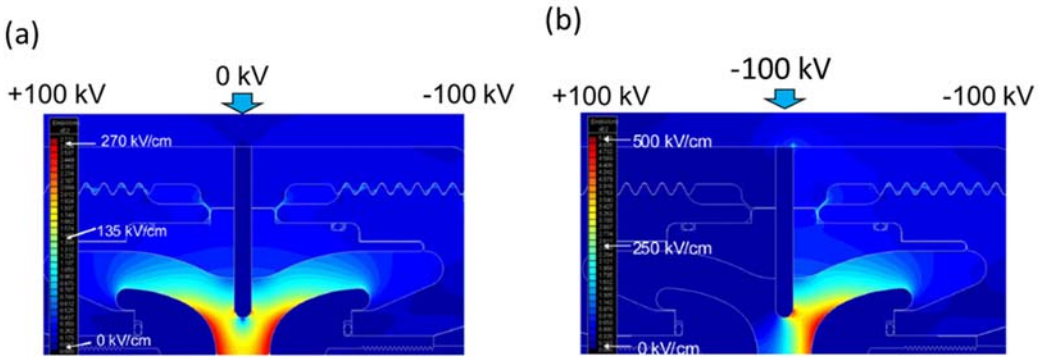

Figure 2.12 Electric field intensities inside Kinetech switch when charged to ±100 kV. Left picture—DC charge with trigger pins at ground. Right picture—fields in the switch when the trigger pins are at +100 kV during the triggering process.

When a trigger pulse is delivered to the trigger pin, the amplitude of the electric field in the switch changes and is shown in Figure 2.12 (b). When -100 kV is delivered to the trigger pin, the voltage between the left side of the blue electrode and the trigger pin is -200kV. The distance between the left electrode and the trigger pin cannot hold the voltage and it will cause breakdown on the left side. After left side breakdowns, the voltage of trigger pin becomes 100 kV, the voltage difference between the electrode and the trigger pin is 200 kV. It cannot hold the voltage and a breakdown occurs. As a result, the spark gap is activated.

2.3.3 Krytrons

A krytron is a low-pressure gas discharge device with a tetrode configuration, sealed in a glass tube with a cold cathode. It operates at 1.3 kPa of helium gas pressure with no gas reservoir. A special design of the anode grid area, together with the applied gas pressure, allows a relativity large hold-off voltage. A short trigger delay time of about 30 ns and fast commutation phase are achieved through an existing plasma created by a glow discharge between a special keep-alive electrode (has a low positive voltage applied) and the cathode [2].

A krytron pack with an integrated trigger transformer is shown in Figure 2.13. The

current and voltage rise times are less than 1 ns and the maximum switch current and voltage are around 3 kA and 8 kV, respectively. A pulse length of up to 10 us and a repetition rate of 1 kHz can be achieved. The trigger plasma spreads into the space between a control grid (trigger input channel in Figure 2.13) and the cathode. Switching is initiated by a positive pulse at the control grid, which, except for a small opening, surrounds the anode. A ^{63}Ni β-emitter is also enclosed in the glass tube. This serves as a weak permanent pre-ionizer such that faultless switching is guaranteed even after a long period of time not being used. It makes the krytron very robust in different environments. A disadvantage is the limited lifetime of 10^6 discharges, which is determined by the gas consumption and the electrode erosion[2].Nevertheless, krytrons are still widely used in fast trigger generators and Pockels cell drivers and also ideal for the detonating circuit in bombs[2].

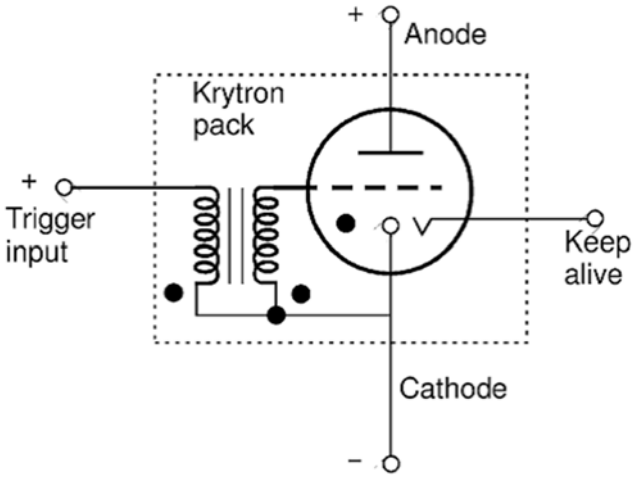

Figure 2.13 Schematic of krytron pack including a trigger transformer.

2.3.4 Solid-state switches

As mentioned previously, the design of the spark gap switch needs a trigger pulse to induce the electrodes breakdown in it. Solid-state switches that can provide fast switching are very suitable to provide a trigger pulse. We use Insulated Gate Bipolar Transistors (IGBT) in our trigger pulse generator. Because the internal structure of IGBT is similar to Bipolar Junction Transistor (BJT) and Metal-Oxide-Semiconductor Field-Effect Transistor (MOSFET), we will introduce BJT and MOSFET first and finally IGBT.

2.3.4.1 Bipolar Junction Transistor (BJT)

Bipolar Junction Transistor are manufactured in two types, NPN and PNP, based on the doping types of the three main terminal regions. The structures are shown in Figure 2.14.

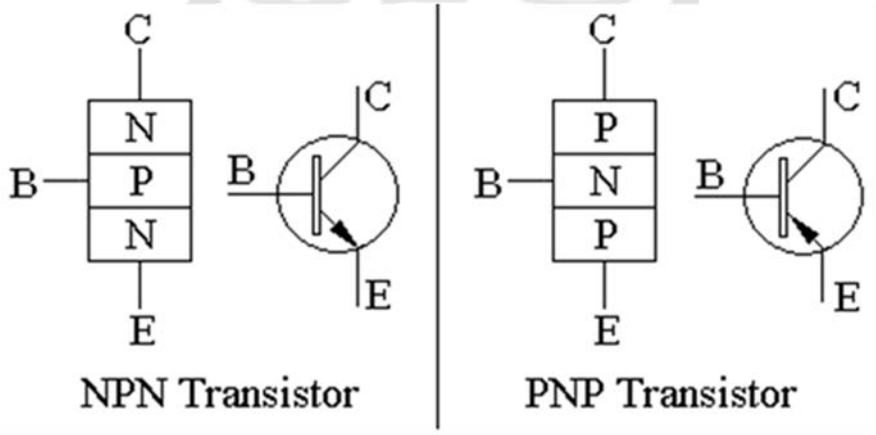

Figure 2.14 The left picture is N-type BJT. The right picture is P-type BJT.

A N-type BJT is a transistor where a p-doped semiconductor is sandwiched between two layers of n-doped semiconductor. Similarly, a P-type BJT is a transistor where a n-doped semiconductor is sandwiched between two layers of p-doped semiconductor. In Figure 2.14, BJT has three pins, Emitter (E), Base (B) and Collector (C). Emitter and Collector are in charge of emitting and collecting electrons and holes. Base is used to control the current flow

from Emitter to Collector. In N-type BJT, when the B-E junction is forward bias and B-C junction is reversed bias, it is in the operation region. Because of the different doping concentration of the Emitter and Base (concentration of Emitter is larger than Base), electrons can cross B-E junction to "Base region", even cross Base region to B-C junction. At the B-C junction, the electric filed will attract electrons to "Collect region". At the same time, holes will cross B-E junction from "Base region" to "Emitter region." The current of the Emitter (I_E) includes electron flow (I_{nE}) (from the Emitter to the Base) and hole current (I_{pE}) (from the Base to Emitter). Because the doping concentration of the Emitter is larger than Base, the electron current is larger than hole current (InE $\gg$ IpE). On the other hands, the current direction in P-type BJT is reversed comparing to N-type BJT. It means that the principle of the operation is also reversed. There are three types of operation modes as shown in Figure 2.15[15] and Figure 2.16[16]: Cutoff mode, Amplification mode and Saturation mode.

1. Cutoff mode: In Figure 2.15, when the voltage between the Base and the Emitter (V_{BE}) is lower than about 0.6V, the current of the Base (I_B) is about 0A, it cannot drive the transistor.
2. Amplification mode: N-type BJT is a forward bias type ($V_{BE} > 0$). In Figure 2.15, when the voltage between Base and Emitter (V_{BE}) is larger than 0.7V, I_B increase dramatically. It means the transistor is driven. By adjusting the value of I_B, one can control the transistor operation. In Figure 2.16, when I_B is kept fixed, I_C does not change by increasing V_{CE}. However, when the V_{CE} value is kept fixed, I_C increases by increasing I_B.
3. Saturation mode: when V_{BE} is kept fixed at 0.7V or slightly higher than 0.7V and the V_{CE} smaller than 0.3V, it is in the saturation region. In Figure 2.16, when V_{CE} changes, I_C changes dramatically. I_C and I_B are not amplified and the characteristic of current

amplified disappears gradually.

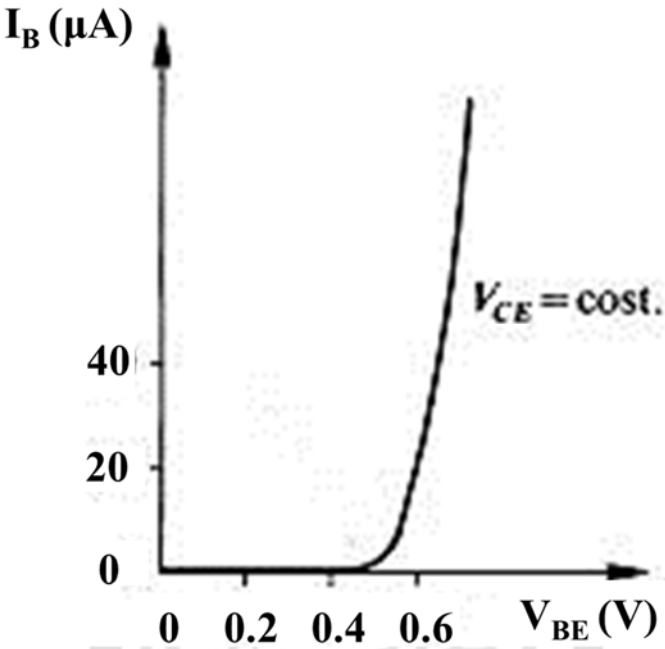

Figure 2.15 N-type BJT. The relationship between current of Base (I_B) and bias of Base and Emitter (V_{BE}).

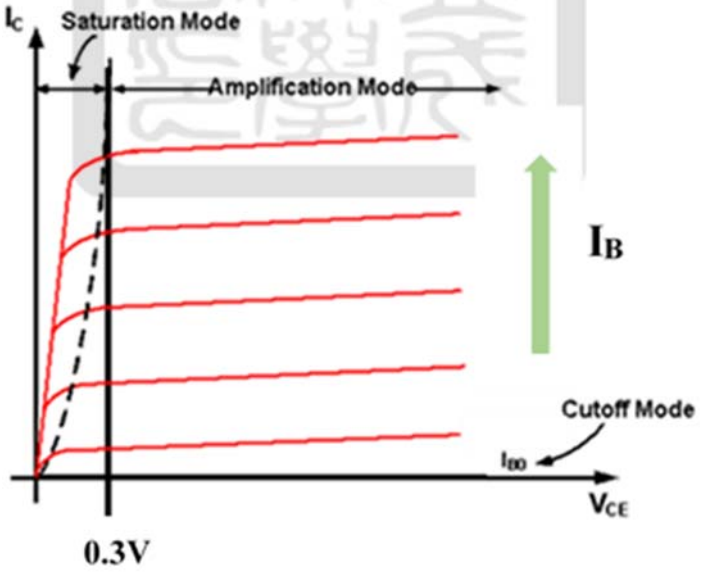

Figure 2.16 Three operation mode of transistor. Cutoff mode, Amplification mode and saturation mode. Different red lines is with different I_B.

2.3.4.2 Metal-Oxide-Semiconductor Field-Effect Transistor (MOSFET)

MOSFET has three pins, Gate, Drain and Source as shown in Figure 2.17. In the circuit symbol, the arrow in the circle to the right direction means the P-type MOSFET or vice versa.

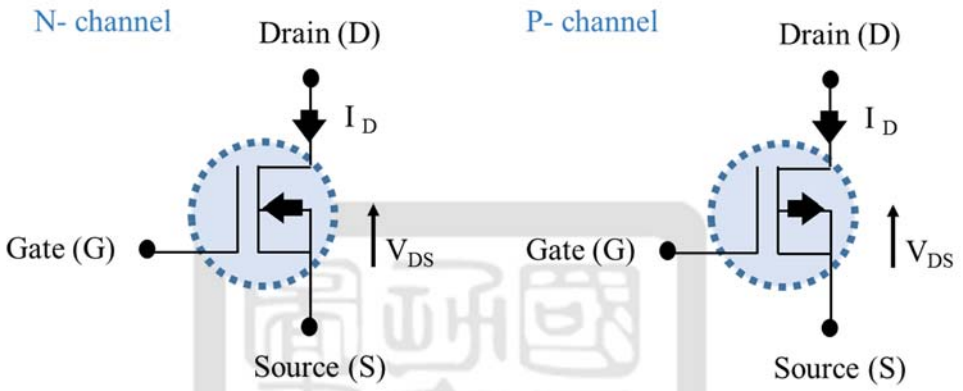

Figure 2.17 N-type and P-type MOSFET.

Figure 2.18[17] is the structure of an N-type MOSFET. There are four layers, Gate, Drain, Source and Bulk. According to Figure 2.18, Gate is a stack of metal, oxide layer and semiconductor. It is similar to the structure of a capacitor. When enough positive voltage is applied to the Gate, the oxide layer will attract conductive electrons and form a channel near the junction with the metal. It can turn on the n^+ channel between Source and Drain. According to this principle, we can control the voltage of Gate to adjust the electric field of oxide layer and control the conductivity between Source and Drain, as shown in Figure 2.19[17]. Which is the characteristics for an N-type MOSFET. There are three types of operation mode: Cutoff mode, Amplification mode and Saturation mode.

1. Cutoff mode: When there is no applied bias on the Gate, the n^+ channel between

Source and Drain is not formed. It is called cutoff mode. When the applied bias voltage increase gradually, the metal layer of Gate accumulates positive charges. The other side of oxide layer attracts the same amount of negative charges. At this moment, the negative charges combine with holes, the current cannot flow through MOSFET. The channel between Source and Drain is not turned on.

2. Amplification mode: When the applied voltage is above the critical voltage at the Gate (between intersections of red line and blue lines are the critical voltage separating different modes), the interface of oxide layer and semiconductor becomes a conductivity layer. At this moment, the channel between Source and Drain turned on by this conductivity layer.

3. Saturation mode: in the range where I_D does not change by increasing V_{DS}.

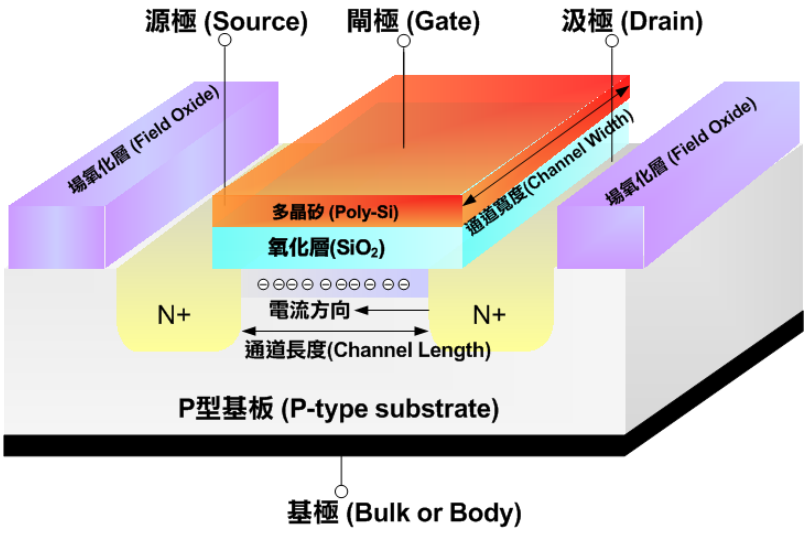

Figure 2.18 N-type MOSFET.

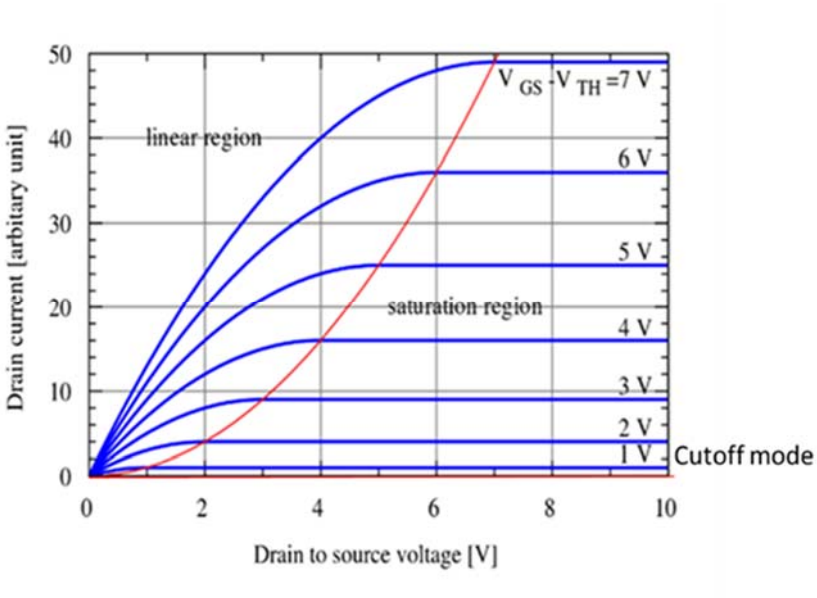

Figure 2.19 Three types of operation mode of MOSFET. Cutoff mode, Amplification mode and saturation mode.

2.3.4.3 Insulated Gate Bipolar Transistor (IGBT)

Insulated Gate Bipolar Transistor is the combination of BJT and MOSFET as shown in Figure 2.20[18].

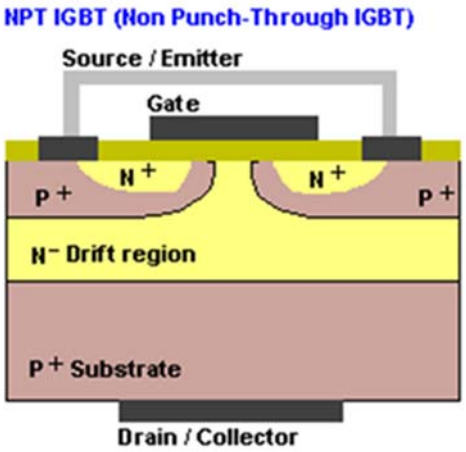

Figure 2.20 NPT IGBT.

The Drain of the IGBT has extra one N^- layer and one P^+ layer compared with MOSFET.

After adding the N^- layer and P^+ layer on the MSOFET, the origin Drain becomes Collector, Source becomes Emitter. Because of the structure, IGBT is considered as the combination of MOSFET and BJT. The equivalent circuit is shown in Figure 2.21[19].

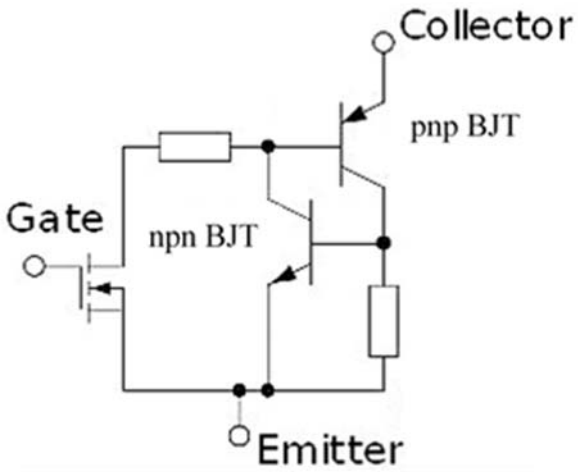

Figure 2.21 Equivalent circuit of IGBT.

In Figure 2.21, there are two BJTs in an IGBT. Because of the structure, it has "Latch-up" effect. A latch-up is a type of short circuit which can occur in an integrated circuit (IC). More specifically it is the inadvertent creation of a low-impedance path between the power supply rails of a MOSFET circuit, triggering a parasitic structure which disrupts proper function of the part, possibly even leading to its destruction due to overcurrent[13]. The key point of controlling the Latch-up effect is to control R_S. Nevertheless, this structure can enhance the capability of driving current. On the other hands, when the channel is turned off in a short period of time, there are some holes flowing into the Collector while there is no electron flow. This phenomenon of IGBT is called tailing current. It will influence on the turn-off time and the working frequency of IGBT. In order to reduce the turn-off time of the tailing current, there is a new technology of adding an extra N+ buffer on the IGBT (shown in Figure 2.22[18]).

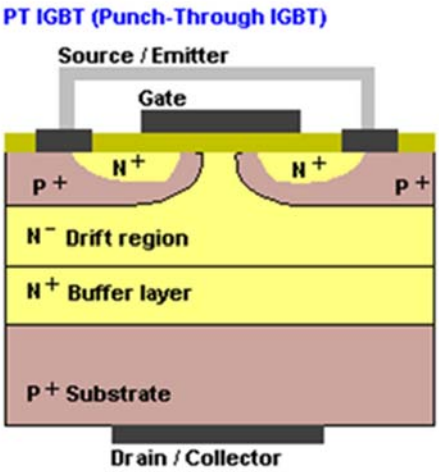

Figure 2.22 PI IGBT.

The current of IGBT is controlled by adjusting the Gate voltage. It is easier than using current to control the IGBT. Therefore, IGBT is more widely used in nowadays. Figure 2.23[20] is the characteristic of operation of the IGBT. There are three types of operation mode: Cutoff mode, Amplification mode and Saturation mode.

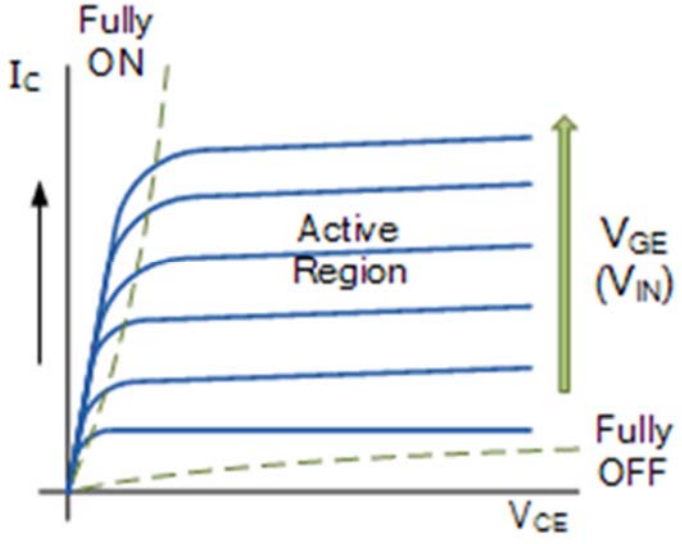

Figure 2.23 The characteristic of operation of the IGBT, there are three types of operation mode: Cutoff mode, Amplification mode and Saturation mode.

1. Cutoff mode: when the voltage between the Gate and the Emitter (V_{GE}) of IGBT is 0V, MOSFET is cut off and the current from P-type BJT will also be cut off. The

transistor cannot be driven.

2. Amplification mode: When the voltage between the Gate and the Emitter (V_{GE}) is positive, the MOSFET is turned on. At this moment, the resistance between the Collector and Base of P-type BJT is reduced, P-type BJT is turned on.
3. Saturation mode: when the voltage between the Gate and the Emitter (V_{GE}) of IGBT reaches a critical value, the voltage will approach saturation and drive the IGBT.

Chapter 3 IMPLEMENTION OF THE PULSED-POWER SYSTEM

The application of the pulsed-power system we proposed is to remove rust in metals. There are several key components that needs to be built. They are a spark gap switch and a trigger pulse generator. Since the expected rise time of the pulsed-power system is ~ 70 ns, the spark gap switch needs to be switched ON in a time much shorter than 70 ns. The rise time of the trigger pulse also needs to be much shorter than 70 ns. The detail design and implemention of the pulsed-power system trigger pulse generator and the spark gap switch will be given in section 3.2 and 3.3, respectively.

3.1 Design of the pulsed-power system

The design shown in Figure 1.3 is replotted in Figure 3.1. It will be built using two 40 nF capacitors charged to ±10 kV. The trigger pulse generator is used to induce the breakdown spark gap switch.

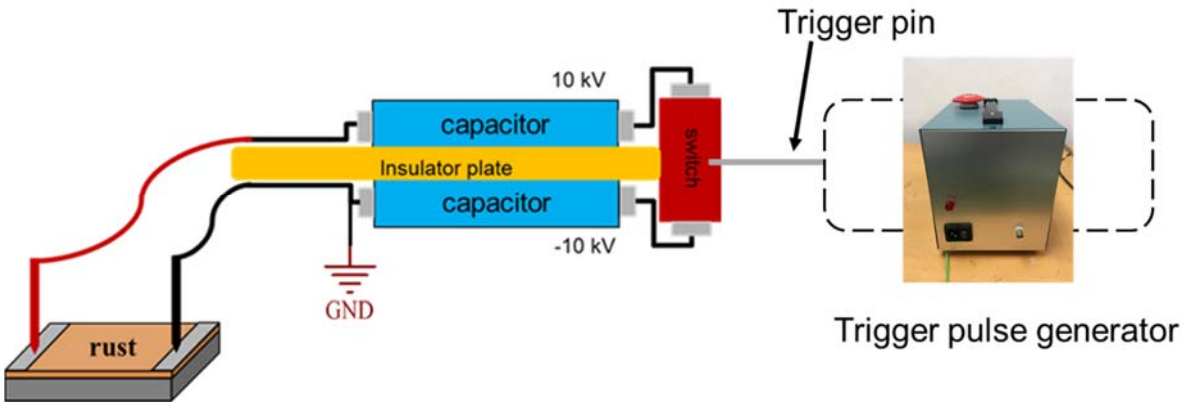

Figure 3.1 The design of the pulsed-power system

Figure 3.2 is the circuit of the pulsed-power system without rusted object. We used +10kV high voltage power supplies (HVPS1) and -10kV high voltage power supplies (HVPS2) to charge each capacitor. Details will be given in the following sections.

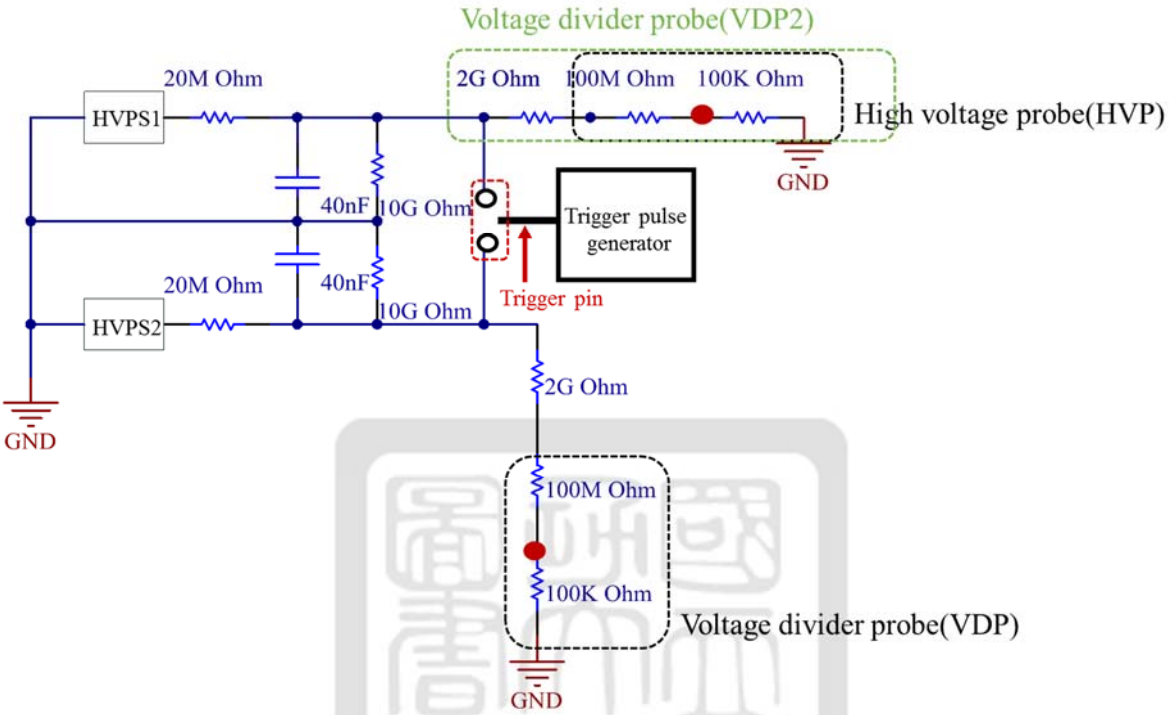

Figure 3.2 The circuit of the rust remover. The red points are testing points. The red dash square is spark gap switch.

3.2 The trigger pulse generator

In order to control the time of breakdown in the switch, a high voltage trigger pulse with short rise time is used. Since our capacitors will be charged to ±10kV, a pulse more than 10 kV is required to induce breakdown in the switch. We implemented two different pulse generators using (1) a Marx generator and (2) an ignition coil for cars. Delay time and jitter defined in Figure 3.3. Figure 3.3 are used to determine the quality of a trigger pulse generator. The delay time is the time difference between the low voltage trigger signal and the beginning of the high-voltage trigger pulse. The jitter is defined as the uncertainty in time of

the beginning of the high-voltage trigger pulse relative to the low-voltage trigger signal, i.e., the standard deviation of the time at the beginning of the high-voltage trigger pulse from many shots.

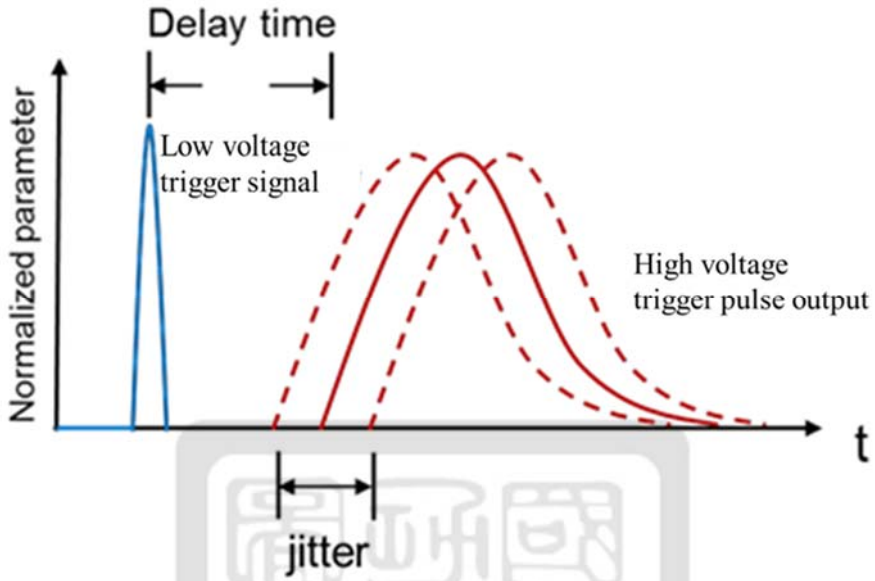

Figure 3.3 Definition of delay time and jitter. Blue line is a trigger pulse and red line is discharge current while switches breakdown. The time between the peak of trigger pulse and the beginning of red line is called delay time. Each time of switch breakdown is a little different. The range of the uncertainty in time is called jitter.

3.2.1 A trigger pulse generator using a Marx generator

A Marx generator using commercial self-breakdown switches can be suitable for generating a high voltage trigger pulse. It is because the turn-on time of a self-breakdown switch can be in the order of nanoseconds. Further, a high voltage output can be generated with a relatively low voltage power supply using a Marx generator. Therefore, we built a three stages Marx generator given in Figure 3.4.

(a)

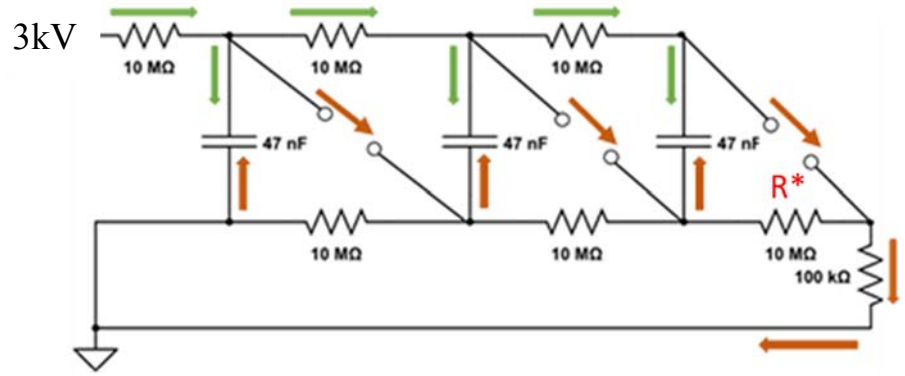

(b)

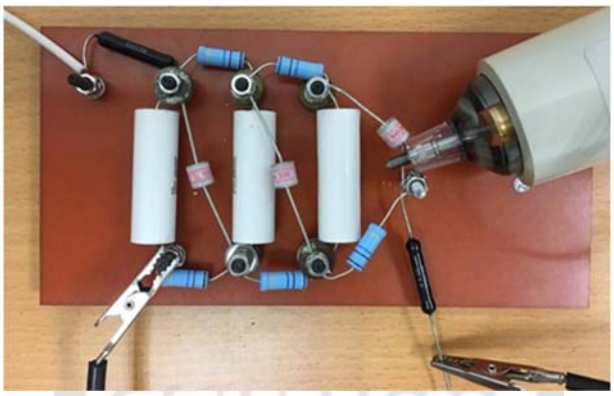

Figure 3.4 (a) A three stages Marx generator. During the charging phase, capacitors are connected in parallel. Current flow follows green arrows and voltage across capacitors increase. When the most left triggered switch can't hold the voltage, it will be closed and the current can flow through it. It is called the discharge phase. At this time, current follows orange arrows. (b) Experimental circuit**.**

Note that R* was accidentally added in the circuit which should have not been installed in a Marx generator. The charging current may flow through R* and thus the load during charging. Nevertheless, it should not make a big difference during discharge due to its high resistance.

In the test of the three-stage Marx generator, a high voltage power supply (S1-10P-L2) was used. The maximum output voltage is 10kV and the power is 1.5 W (1 W is for safety). According to $P = \frac{V^2}{R}$, the resistance is 10MΩ to protect the power supply. Nevertheless,

only 3 kV is used. An output of 7kV was delivered while the charging voltage was only 3kV. The result of the output is given in Figure 3.5. The energy may be lost in resistors so that the output voltage was not exactly 9Kv (3x3kV). In Figure 3.5, the voltage increases in three discontinuous steps pointed out by arrows with numbers. They are the characteristics of sequential breakdown of each switch.

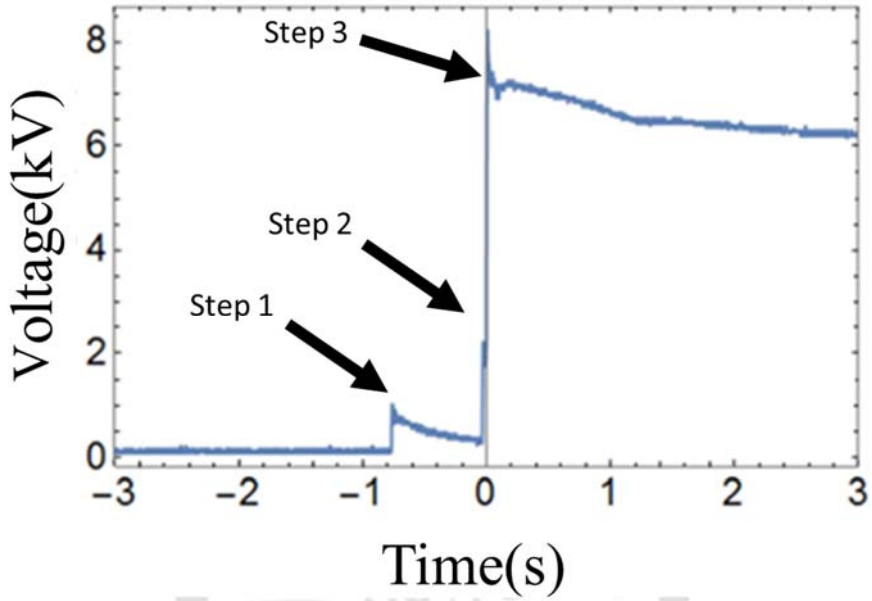

Figure 3.5 Marx generator output voltage vs time. There are three steps of voltage superposition. The rise time of voltage at t~0 is about 4.0 ± 0.5 ns.

One of the triggered switches was replaced with an Insulated Gate Bipolar Transistor (IGBT) because the time of the breakdown couldn't be controlled in the previous design. The IGBT was driven by a circuit introduced in section 3.2.2. Figure 3.6 shows a negative-output Marx generator with controllable triggered switch. The 10 MΩ resistor is for protecting the power supply (S1-10P-L2). The maximum output voltage is 10kV and the power is 1.5 W (1 W is for safety). According to $P = \frac{V^2}{R}$, the resistance is 10MΩ.

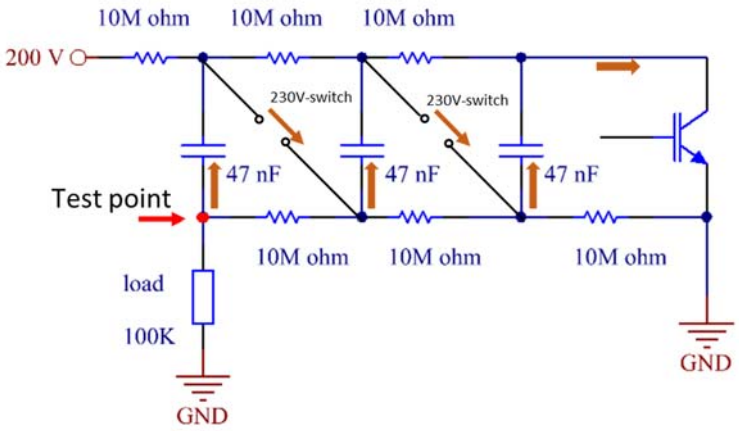

Figure 3.6 Marx generator with controllable triggered switch (IGBT). IGBT and transformer

A square pulse from a function generator is used to control triggered switch (IGBT) being turned ON or OFF. When the IGBT is turned ON, other self-breakdown switches are activated sequentially and the current can flow through it. It is called the discharge phase. At this time, the current direction follows orange arrows. Figure 3.7 shows the test result of three stages Marx generator with controllable triggered switch. In the figure, black line is the square pulse from the function generator and the blue line is the voltage at the test point in Figure 3.6. Similar to Figure 3.5, the voltage increased in three discontinuous steps. They are again the characteristics of sequential breakdown of each switch.

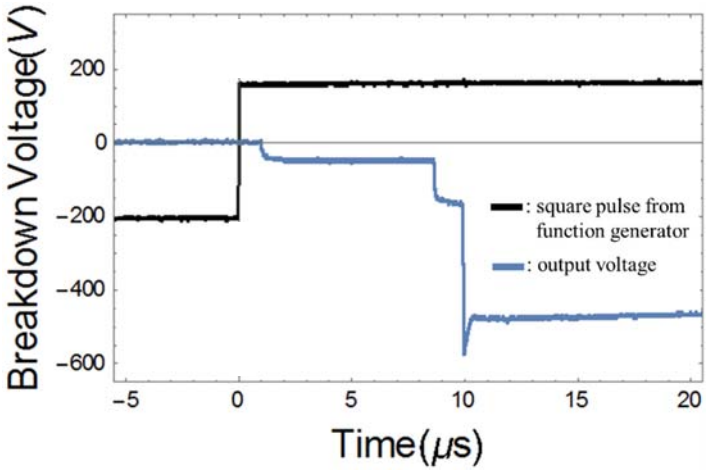

Figure 3.7 Three stages Marx generator was tested and voltage of output curve revealed three breakdown stages.

In order to remove those steps, we added a self-breakdown switch which can hold 400V as shown in Figure 3.8 and the result of test is shown in Figure 3.9. In Figure 3.9, the delay time and the jitter are 22.2μs and ±0.7μs, respectively. We can see that there are no big step in the blue line comparing to the one in Figure 3.7.

Test results show that the Marx generator can provide a reliable trigger pulse. However, if we want to use a Marx generator to output 20kV from a 24V input voltage, we need to use more than 800 stages. The size of the Marx generator is too large. In the following section, a trigger pulse using an ignition coil for cars will be introduced.

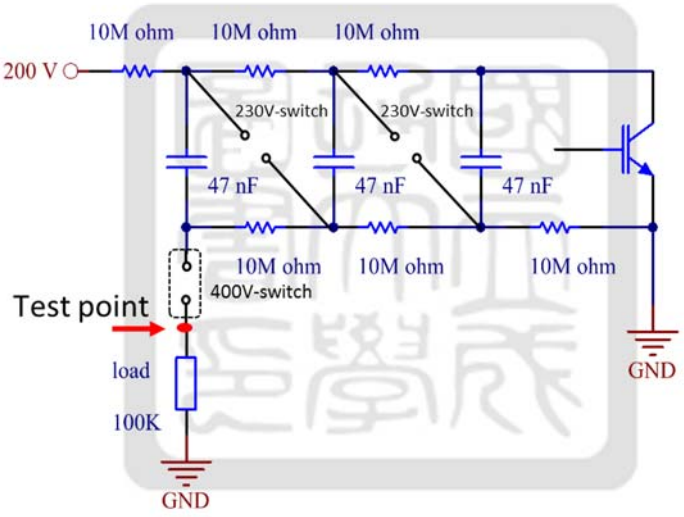

Figure 3.8 Three stages Marx generator with 400V-switch was tested.

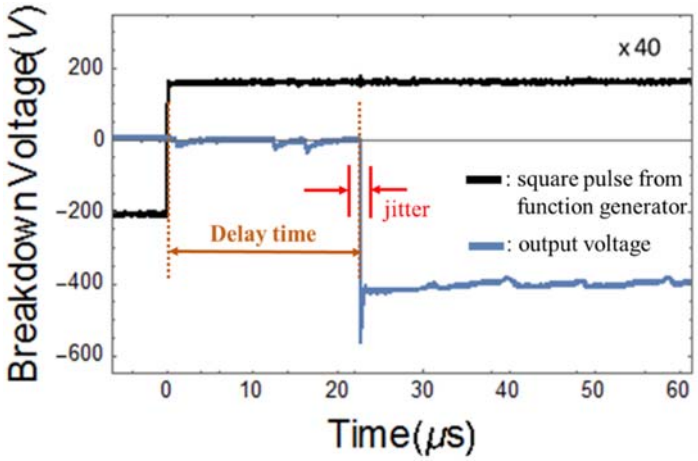

Figure 3.9 The result of the Marx generator with 400V-triggered switch.

3.2.2 A trigger pulse generator using an ignition coil for cars

Figure 3.10 is the design of the trigger pulse using an IGBT and an ignition coil for cars, i.e., a transformer, to generate a high-voltage pulse. The principle of generating the high voltage pulse is that energy is first stored inductively in the primary coil of the ignition coil. A high voltage pulse is then generated at the secondary coil when the circuit is suddenly open.

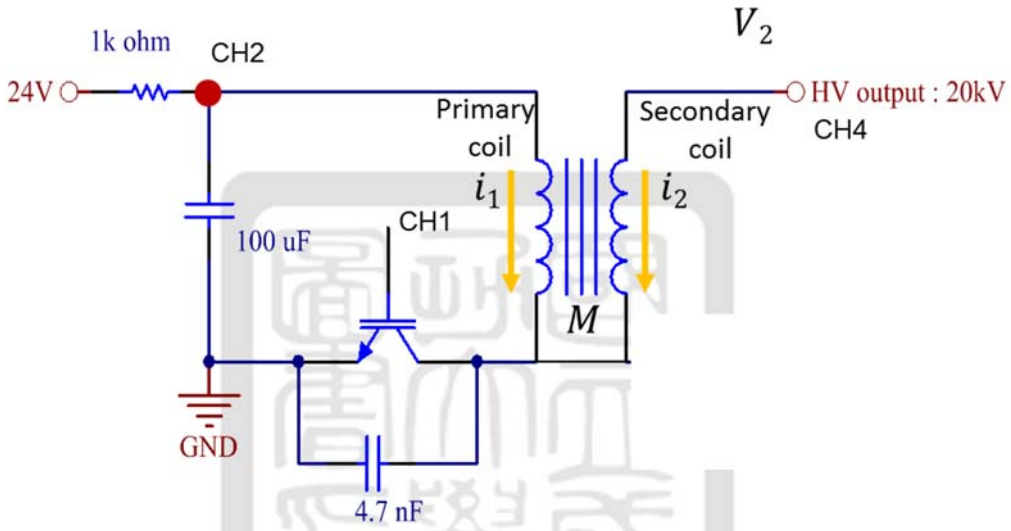

Figure 3.10 The design of trigger pulse circuit. By using square signal to control IGBT turn-off, when a 24 V input this circuit and it can output 20 kV.

When the IGBT controlled by a square pulse from a function generator is ON, the capacitor will begin to discharge and current flow through the IGBT will gradually increase. When the IGBT is OFF, it is open and no current can flow through it. Since the current i_1 drops to zero in a very short period of time (in the order of micro-second), a high voltage $V_2=M\frac{di}{dt}$ where M is the mutual inductance is induced. Notice that dt is determined by the switch OFF time of the IGBT. On the other hands, $di_1 = 0 - i_1 = -i_1$, where i_1 is the discharge current when IGBT is ON. Notice that the 100 μF capacitor and the primary coil of the

ignition coil form a simple RLC circuit. The current oscillates during the discharge. In order to get larger$|di_1|$, i.e., $|i_1|$, the IGBT needs to be turned OFF at the time $|i_1|$ is at maximum. According to this principle, we adjusted the width of the square pulse until the highest output voltage (V_2) occurred. As the result, the width of the square pulse equals to 1.25 ms has the highest output V_2. On the other hand, our trigger pulse circuit didn't have the 4.7 nF capacitor initially. But when we did the experiment, the IGBT was damaged. The oscillation of current damaged the IGBT since IGBT cannot hold large reversed current. When the 4.7 nF capacitor is added, the fast oscillation occurs, the current flows through the capacitor not the IGBT so that the IGBT is protected.

To drive the IGBT (GT60M324), a voltage of 15V is needed. In other words, it can't be driven directly from a TTL signal. A gate driver (FOD3184-V507D) is used. Figure 3.11 is the driving circuit of the IGBT. We used a DC-DC convertor (DCW05A-15) to drive the gate driver and thus the IGBT. We used 24V AC-DC power supply to drive the DC-DC convertor and provide a ±15V output to the gate driver. The square pulse from a function generator will be used to control the ± 15V gate output to the IGBT and turn IGBT ON or OFF. The gate driver also isolates the potential high voltage noise from the IGBT optically. However, it is not enough and the function generator may be damaged. Therefore, an additional protection using the optical coupling is used.

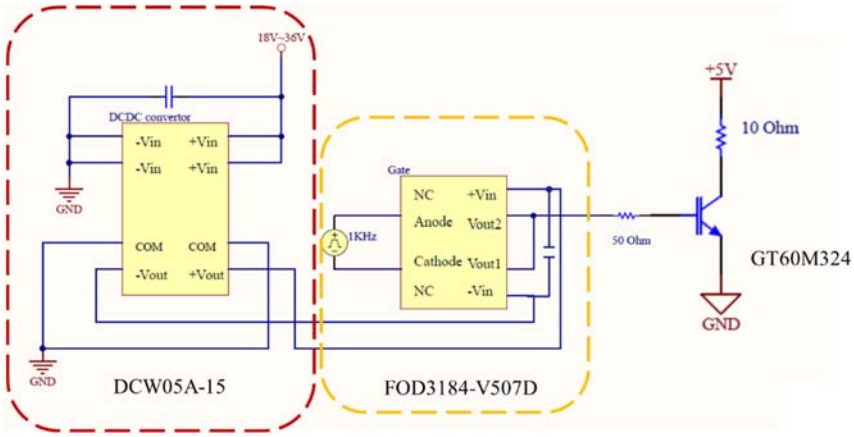

Figure 3.11 The driving circuit of IGBT.

Figure 3.12 is the circuit of the optical coupling [12] used for protecting our function generator. The pulse from the function generator is connected to the “Data_IN” of the fiber coupling (HFBR-3810Z) first and finally come in the gate driver which at P2 in Figure 3.12. An optical isolated pulse delivered from the “Data_OUT” to the Anode of the gate driver in Figure 3.11.

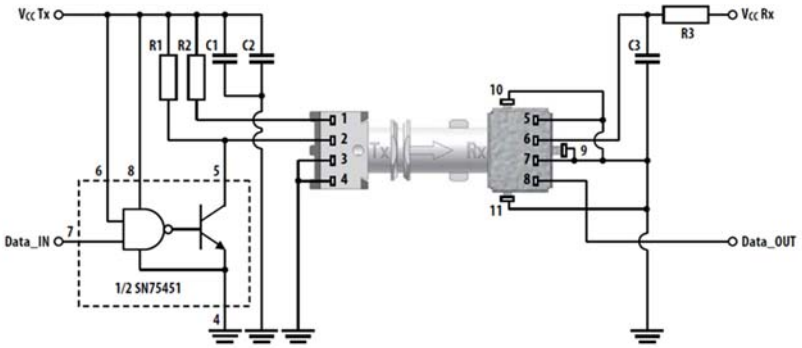

Figure 3.12 The circuit of the fiber coupling.

Figure 3.13 is the layout figure of trigger pulse circuit by using Altium Designer[21]. We used this design to layout to the Printed circuit board (PCB) by ourselves. Square shape at P1 is 24V input channel, circle shape at the P1 is ground, Square shape at P2 is square pulse from function generator, circle shape at the P2 is ground, C1 is 1 μF capacitor, C2 is 0.1 μF capacitor, C3 is 100 μF capacitor, C4 is 4.7 nF capacitor, R1 is 220 Ω resistor, R2 is 51 Ω resistor, R3 is 1k Ω resistor, U1 is DC-DC convertor (DCW05A-15), U2 is a gate driver ((FOD3184-V507D), Q1 is IGBT (GT60M324).

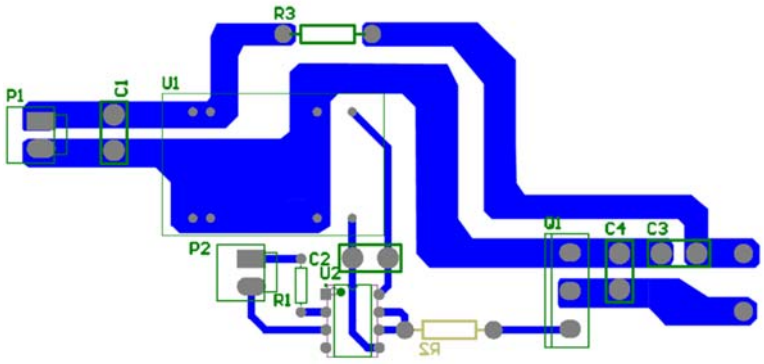

Figure 3.13 The layout figure of trigger pulse circuit by using Altium Designer.

Figure 3.14 is the trigger pulse generator. There are three circuit board: optical coupling circuit board and an IGBT circuit board and an ignition coil for car. There are two output power supplies 24V output power supply is for DC-DC convertor which is in the IGBT circuit board, 5V output power supply is for optical optics which is in the optical coupling circuit board.

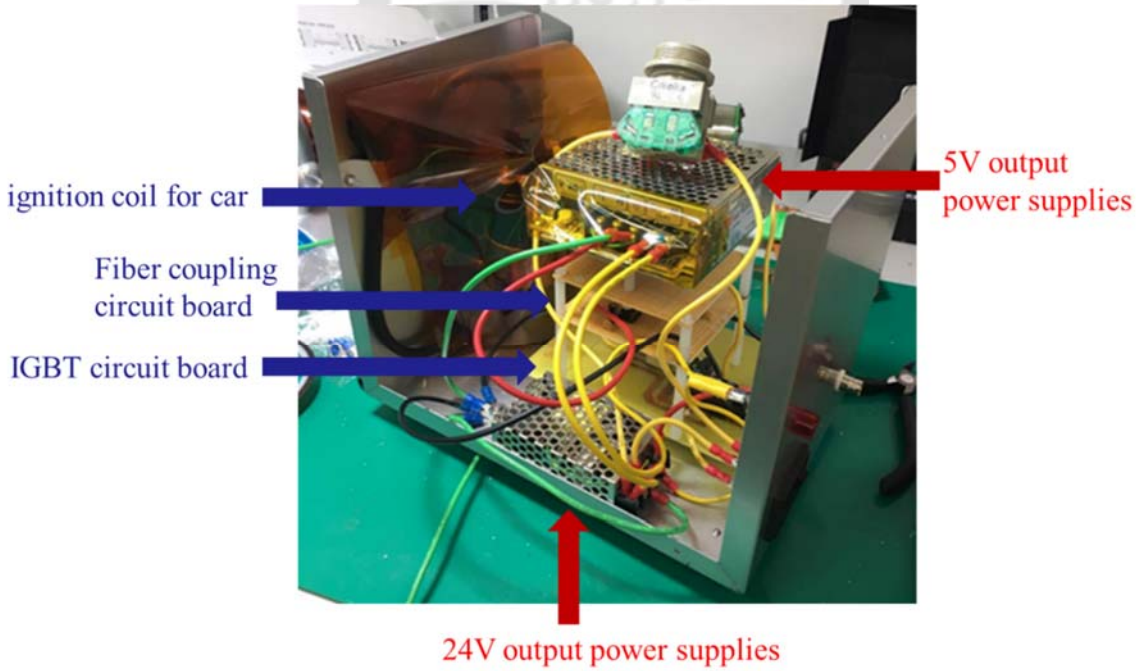

Figure 3.14 Trigger pulse generator.

As shown in Figure 3.15, a high voltage pulse of more than 20 kV with a rise time of 55 μs and a jitter is 0.4 μs is generated. It is the trigger generator we use for the pulsed-power system.

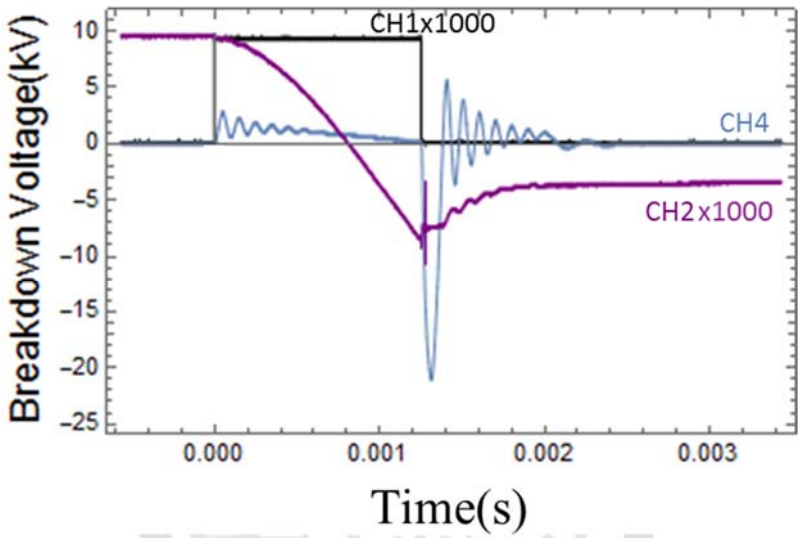

Figure 3.15 The result of trigger pulse by using IGBT and transformer. The black line (CH1) is the square pulse (400 Hz) from the function generator, the blue line (CH4) is the output voltage (V2) and the purple line (CH2) is the voltage of the capacitor.

3.3 The spark gap switch

The switch we built is shown in Figure 3.16. The material of the tube is acrylic. The length is 11 cm and the outer diameter and the inner diameter are 6 cm and 4 cm, respectively. There are one pair of screws with corn nuts as electrodes and a small screw with corn nuts as a trigger pin. The distance between two electrodes and the location of the trigger pin are adjustable. In our system, the distance of the gap between two nuts needs to hold ~ 20kV in air and the relationship between the voltage and the distance of the gap is tested.

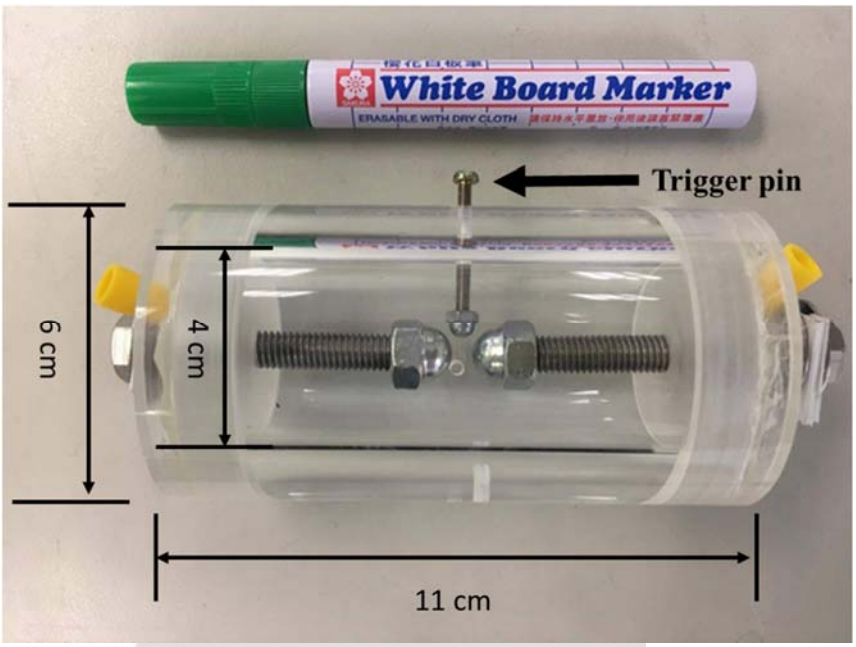

Figure 3.16 The design of the switch

3.3.1 Calculated gap distance using different gas in the switch

It is very important to know the required gap distance in a switch to hold a corresponding voltage. We can estimate the distance between two electrodes using Paschen curve

$$V_b = \frac{B*P*d}{\mathrm{Log}\left[\frac{A*P*d}{\mathrm{Log}\left[1+\frac{1}{\gamma}\right]}\right]} \tag{3.1}$$

where A is the ionization, B is a constant related to the excitation and ionization energies, P is gas pressure and d is the distance of the gap between two metals[7]. Two different gases, Air and SF_6, are considered. The relation between gap distance and breakdown voltage using two different gases are given in Figure 3.17 [5]:

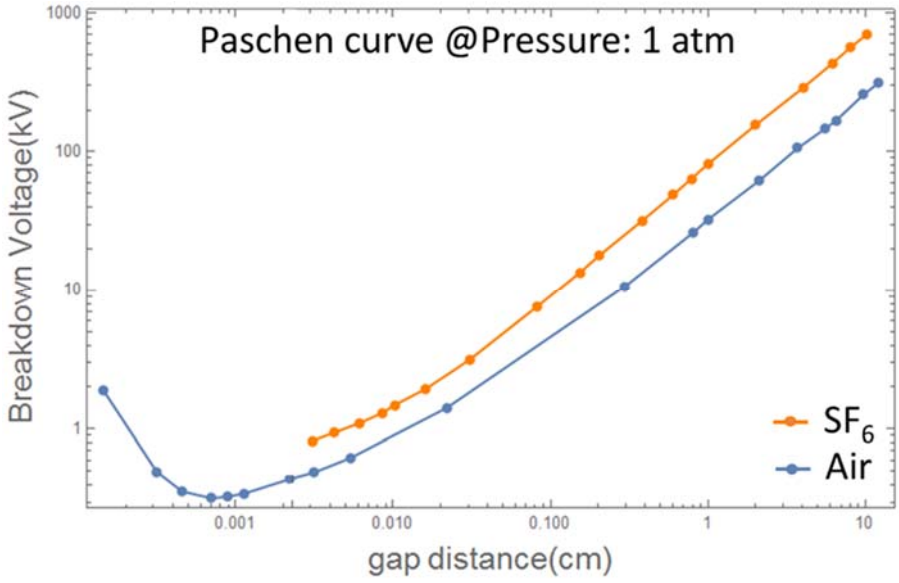

Figure 3.17 Paschen curve for Air and SF_6

Equation (3.1) can be written as

$$V_b = \frac{Bpd}{\ln[pd/k]} \tag{3.2}$$

where

$$k = \ln[A/\ln(1+\frac{1}{\gamma})] \tag{3.3}$$

with constants A and B given in Table 3.1 for different gases[5]. To simplify, k is written as a function of pd given in Table 3.2.

Table 3.1values of constants A and B in equation 3.2 and 3.3 for different gases

Gas	A, ionization/kPa-cm	B,V/kPa-cm
Air	112.50	2737.50
SF_6	95.25	2189.25

Table 3.2 computed k in equation 3.2 and 3.3 as a function of pd

Gas	pd (kPa-cm)	k
Air	0.0133-0.2	$2.0583(pd)^{-0.1724}$
	0.2-100	$3.5134(pd)^{0.0599}$
	100-1400	4.6295(corresponding to pd=100kPa-cm in $k=3.5134(pd)^{0.0599}$
SF_6	0.3-3	$\ln[4.1227(pd)^{-0.4331}]$
	3-1200	$\ln[6.4541(pd)^{-0.8374}]$

At 1 atm ($\approx 10^5 pa$), the expected distance that can hold 20 kV between two electrodes using SF_6 and Air in the switch are 0.2 cm and 0.54 cm, respectively. Note that the Paschen curve was obtained using two flat electrodes. With larger electrodes curvature, the distance between the gap may be larger to hold the same voltage. Since the gap distance is shorter by using SF_6, it is more suitable for our pulse-power system. Nevertheless, we don't have a good seal in our switch so that air is used.

3.3.2 Measurement of the relationship between the Breakdown voltage and gap distance of the switch

In our pulsed-power system, capacitors are charged to ±10 kV. Before the trigger pulse is delivered to the switch and induce breakdown in the switch, it needs to hold 20 kV. Therefore, the relationship between breakdown voltage and gap distance of the switch needs to be tested till V=20 kV.

3.3.2.1 DC breakdown voltage vs gap distance

We adjusted the gap distance of switch and increase the voltage until the switch breakdown. To change the distance between the gap, we used spacers with 0.3 mm in thickness in back of the screw to adjust the distance as shown in Figure 3.18. Figure 3.18 (a)

is the 0.3 mm spacer and (b) shows where spacers are inserted to adjust the gap distance. Figure 3.19 is the circuit of using DC power supplies to test the relationship between breakdown voltage and the gap distance of the spark gap switch. Notice that the high voltage probe (HVP) and its internal resistance is also given in the figure. In this case, the DC power supplies (S-10P-L2, Matsussada) provides a voltage up to +10kV. The 100MΩ is for protecting DC power supplies. We can only measure +5kV maximum. (Our high voltage probe resistance is about 100MΩ). The test result is shown in Figure 3.20. We can only measure two points under +5kV.

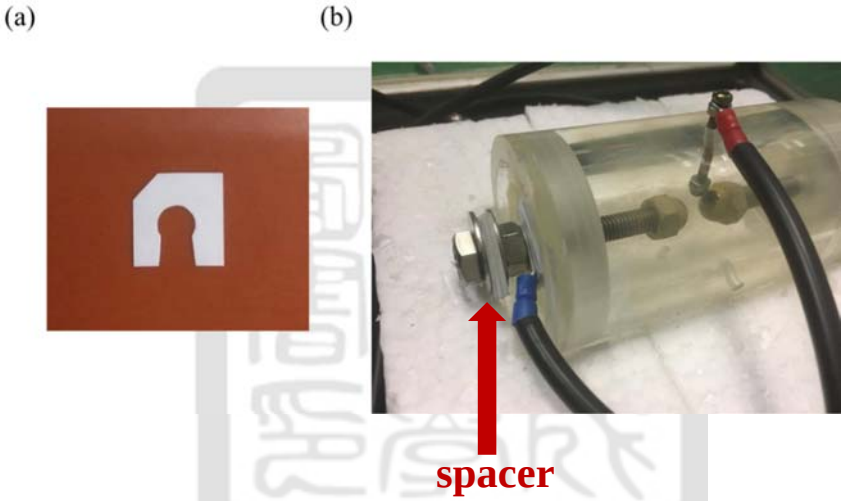

Figure 3.18 (a) 0.3 mm spacer (b) using spacer to adjust the gap distance.

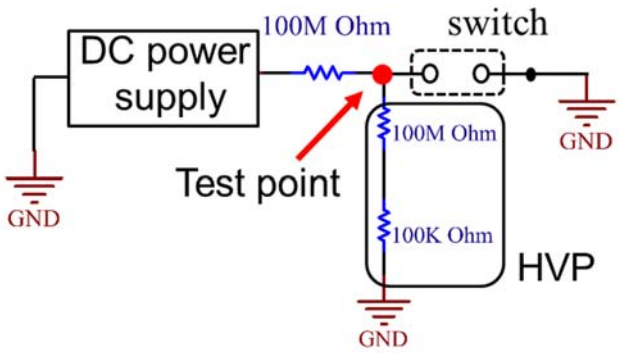

Figure 3.19 The circuit of testing breakdown voltage of DC power supply and the gap distance of spark gap switch.

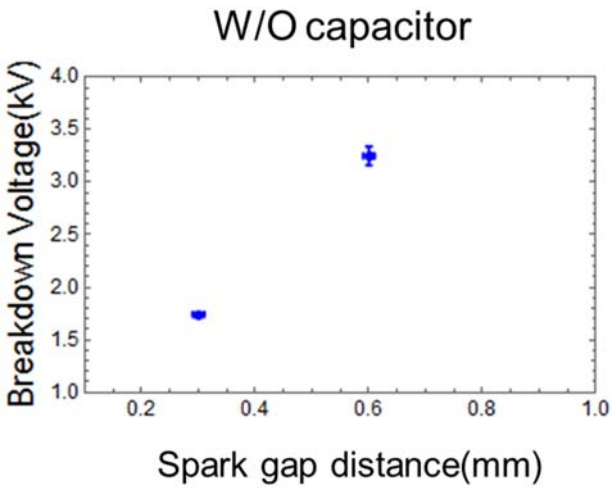

Figure 3.20 The test result of using DC power supplies to test the relationship between breakdown voltage and gap distance of spark gap switch.

In Figure 3.21 is the circuit of testing DC power supplies and spark gap switch with a capacitor connected in parallel to the gap, when discharge happens, it is the capacitor that provides the energy so that the discharge current can be larger. We used 3nF or 40nF to test the relationship between the DC breakdown voltage of the DC power supplies and gap distance of the spark gap switch, respectively. The test result is shown in Figure 3.22, the relationship between breakdown voltage and the gap distance with 3 nF and 40 nF are on top of each other. The result shows that the different capacitance does not affect the relationship between DC breakdown voltage and gap distance. Data in Figure 3.20 is also plotted in Figure 3.22 for comparison, DC voltage can hold higher voltage without capacitor than with capacitor with same gap distance. It is because the capacitor can provide higher current then the DC power supply.

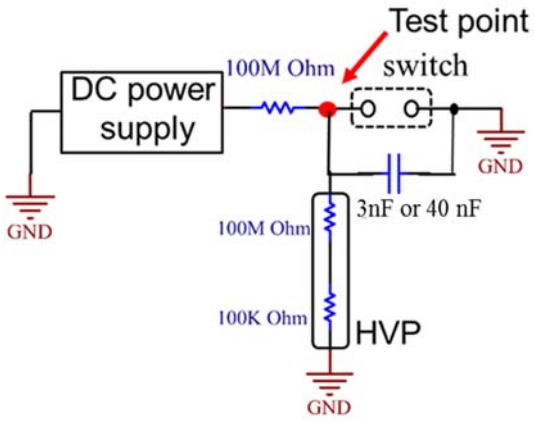

Figure 3.21 The circuit of testing DC power supplies and spark gap switch.

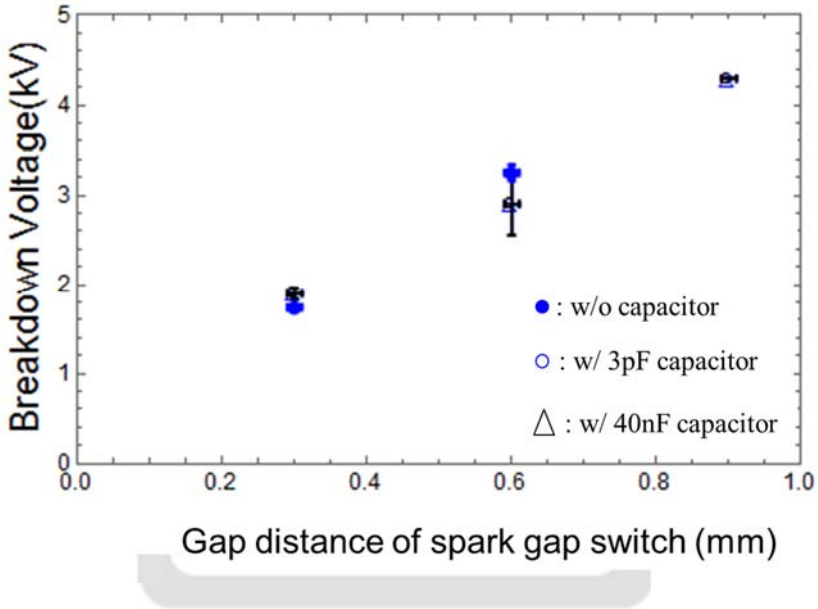

Figure 3.22 The relationship between breakdown voltage and gap distance. The figure include using 3 nF and 40 nF to test the relationship between breakdown voltage and gap distance.

3.3.2.2 Breakdown voltage from the trigger pulse vs gap distance

We need to know the relationship between breakdown voltage and the gap distance when the voltage is provided by the trigger pulse generator. It is to ensure that after a trigger pulse is delivered to the spark gap switch, it can induce a breakdown. Figure 3.23 is the circuit of testing trigger pulse and the spark gap switch.

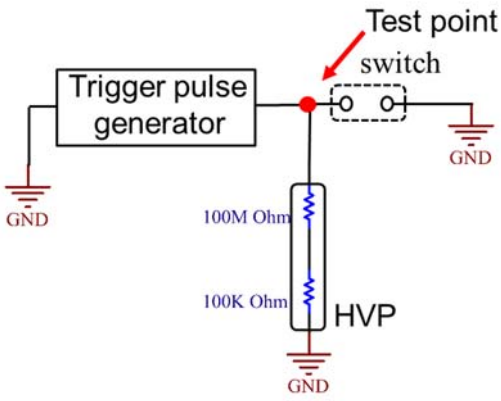

Figure 3.23 The circuit of testing trigger pulse and spark gap switch.

In Figure 3.24, the relationship between breakdown voltage from trigger pulse generator and the gap distance is shown. Comparing to Figure 3.22, to induce breakdown using a short pulse requires a much higher voltage. To induce a breakdown at ~20 kV, a distance less than 4 mm is required.

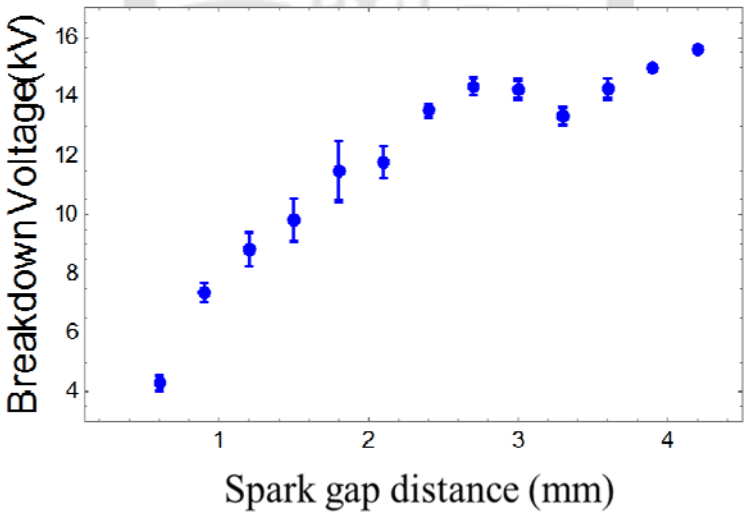

Figure 3.24 The relationship between breakdown voltage of trigger pulse and spark gap switch.

3.3.2.3 Calibration of homemade high voltage probe

When we measured the voltage, we used the high voltage probe P6015a from Tektronix which has a finite input resistance. To protect the high voltage power supply, a resistor is added in the circuit. These resistors are comparable to each other so that the voltage at the test point in Figure 3.19 and Figure 3.21 is lower than the output voltage from the high voltage power supply. The easy solution is to add a resistor connected in series to the high voltage probe. However, the new "probe" needs to be calibrated. Figure 3.25 is the circuit for the calibration. HVPS1 and HVPS2 in Figure 3.26 are the high voltage DC power supplies, square are the points that need to be measured and red points are the test point. The "High voltage probe" (HVP) is a high voltage probe P6015a from Tektronix [11] and "voltage divider probe" (VDP) is made by ourselves. "Voltage divider probe (VDP2) is the modification of HVP. Both VDP and VDP2 need to be calibrated. Notice that two power supplies provide $\pm V_0$ where V_0=0~ 10kV so that voltage across the spark gap is $2V_0$. The maximum power of each HVPS 10W so that 20MΩ resistors are used to protect the HVPS. The resistance is picked such that the maximum power P= $\frac{V^2}{R} = \frac{(10k)^2}{R} = 5 \leq 10$ W. On the other hand, 10 GΩ shunt resistor are used for safety. The energy in capacitors can slowly discharge through the shunt resistor whenever the HVPS is off. Because the capacitor may store energy by the electric collision in air, the 10 GΩ shunt resistor is to release the energy.

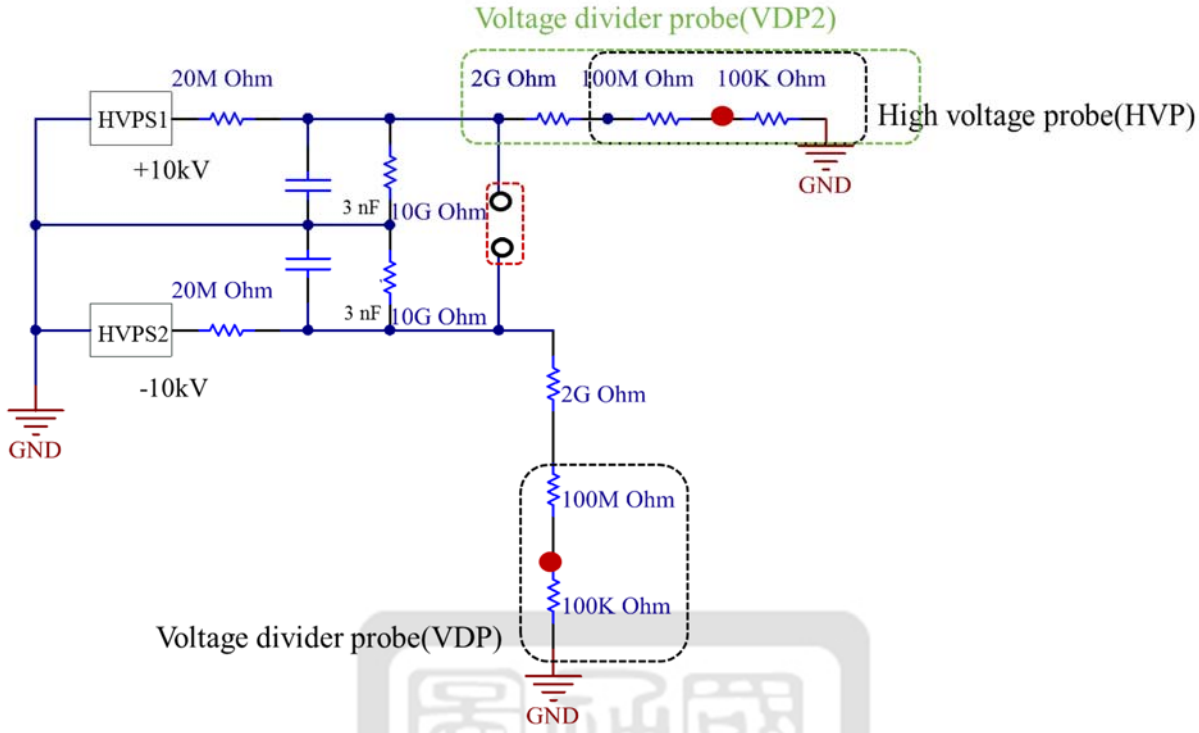

Figure 3.25 The circuit of testing relationship between breakdown voltage and gap distance of switch.

In Figure 3.26, notice that 20M Ω resistors are comparable to the resistor in the high voltage probe (100MΩ) leading to a voltage divider effect. The voltage at point A is only 83% of V_0. A 2G Ω resistor is used to resolve the issue, i.e., $V_A=\frac{2G+100M+100K}{2G+100M+100K+20M}V_0 \approx V_0$. However, we need to calibrate the voltage divider probe (VDP) (with 2 GΩ) and voltage divider probe 2 (VDP2) we made. The process is divided into two parts:

(1) First, we used HVP to calibrate VDP by measurement the same test point at positive output as Figure 3.26.

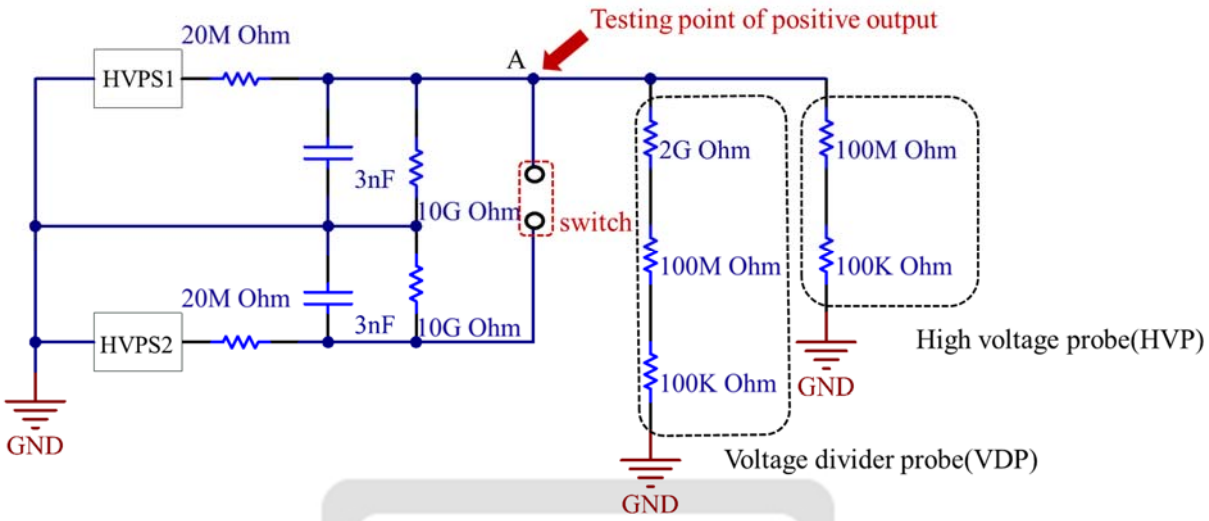

Figure 3.26 The circuit of calibration point.

Figure 3.27 shows the relation between voltage value from HVP and VDP. The fitted formula of the points is

$$V(kV)= (-0.80\pm 0.02) + (24.50\pm 0.08\ )V. \quad (3.4)$$

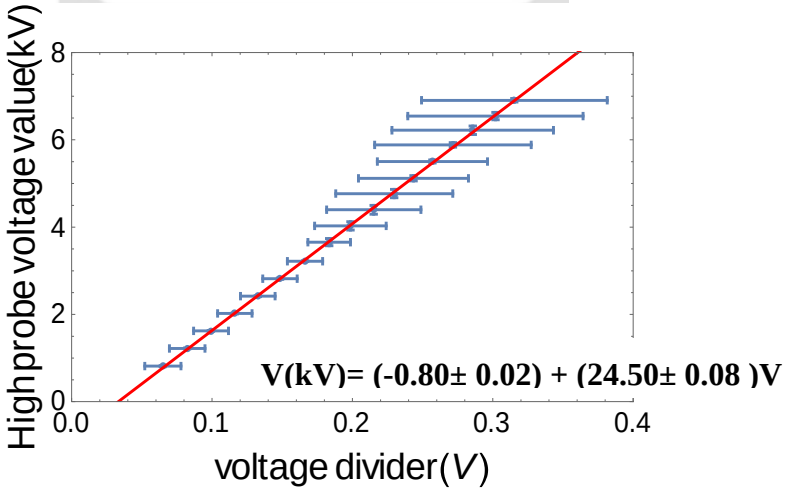

Figure 3.27 Voltage value of HVP and VDP.

(2) Second, we used the VDP to calibrate high voltage probe2 consist a 2 GΩ and HVP connected in series (VDP2) (testing the same point on the testing point of positive output) as shown in .

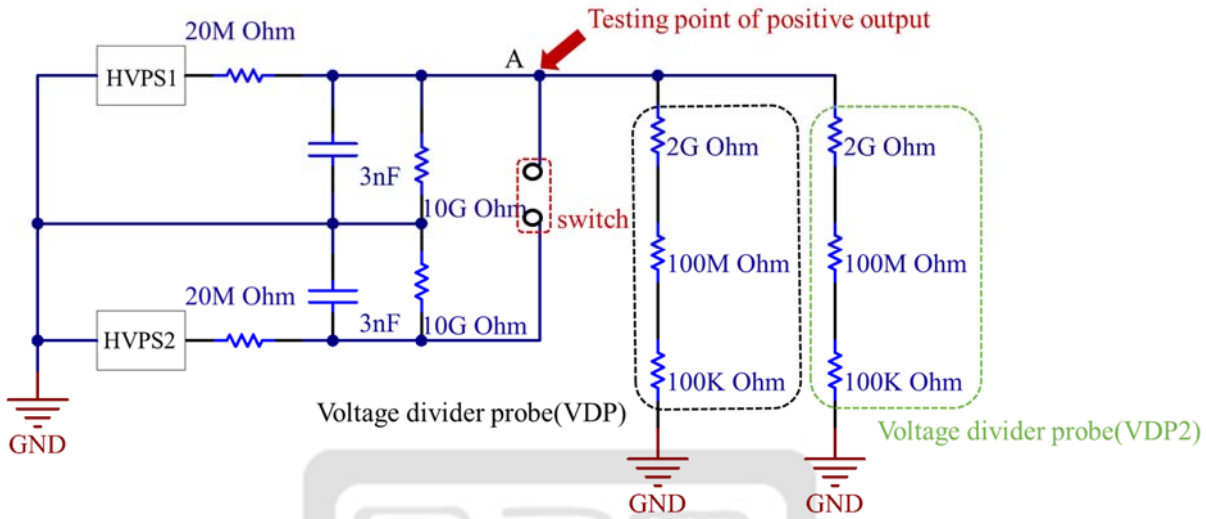

Figure 3.28 The circuit of calibration point

Figure 3.29 shows the relationship between voltage values from VDP2 and calculated voltage from VDP. The fitted formula of the points is

$$V(kV)= (-0.52\pm 0.02)+ (21.8\pm 0.1)\ V. \qquad (3.5)$$

A discontinuity occurs above 7kV. There may be some leaking current through the resistor after 7 kV(VDP).

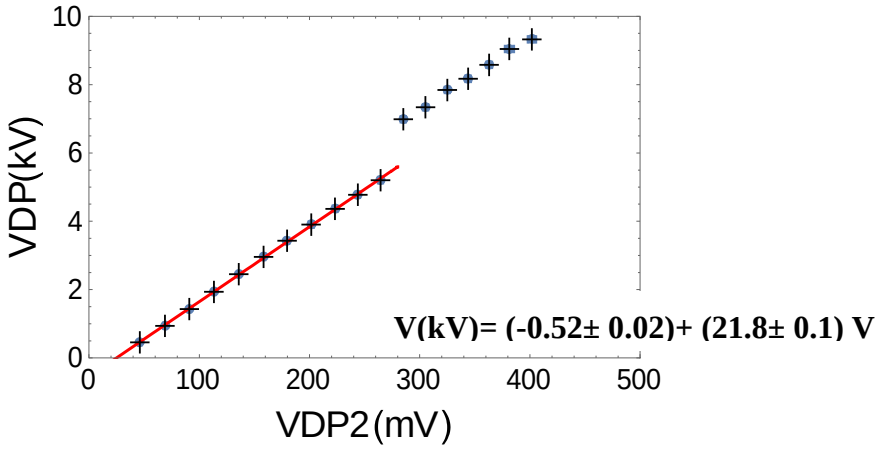

Figure 3.29 Voltage value of VDP and VDP2.

3.3.2.4 DC breakdown voltage above 5 kV vs gap distance

After using the homemade high voltage divider, the voltage across the spark gap can now be higher. Further, two high voltage power supply providing $\pm V_0$ are used. Therefore, more than 10 kV across the spark gap can be provided. Figure 3.29 is the relationship between breakdown voltage above 10kV and gap distances. The testing circuit is similar to the one in Figure 3.25. We can use this test result to design our gap distance of the spark gap switch with trigger pin. The detail will be discussed in section 3.3.2.5.

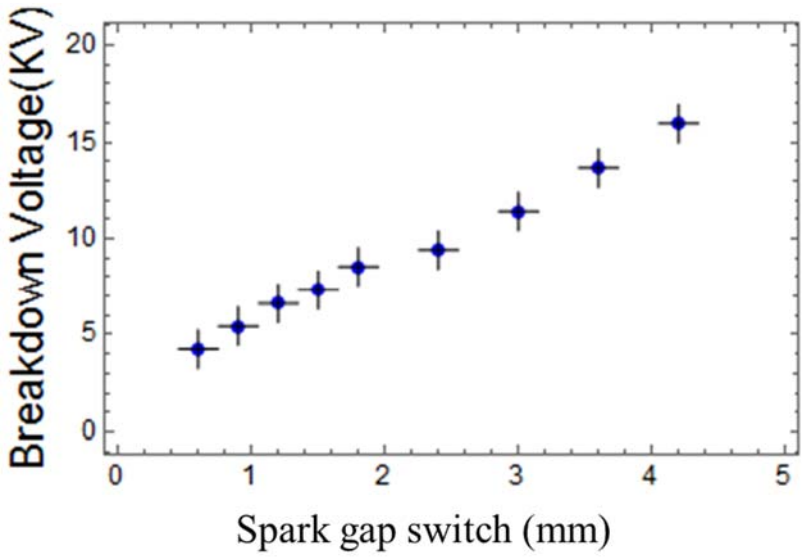

Figure 3.30 The relationship between breakdown voltage and gap distance of spark gap switch.

3.3.2.5 Implementation of the controlled spark gap switch

After testing breakdown voltage using DC power supplies and trigger pulse generator, the distance between electrodes and the trigger pin in the spark gap switch can be determined.

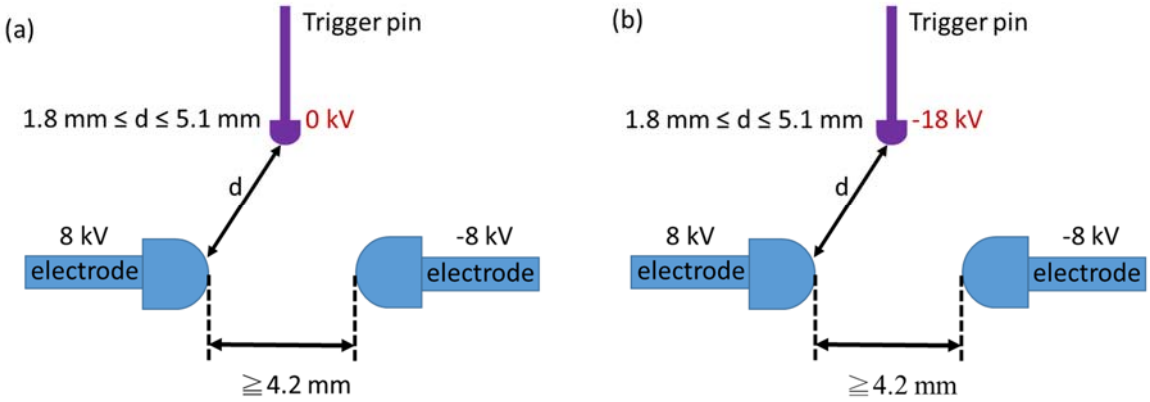

Figure 3.31 The design of the distance of electrodes and trigger pin (a) is before activation, (b) is after activation.

We tested our system only at 16 kV. Figure 3.31 (a) is before the activation. According to Figure 3.30, we know that a 4.2 mm gap between two electrodes can hold about 16 kV. Before the activation, the voltage of trigger pin is 0V, it means that the distance between trigger pin and each electrode of one side needs to hold 8 kV. According to Figure 3.24, the distance between the trigger pin and each electrode must be larger than large 1.8 mm before activation. In Figure 3.31 (b), when the -18kV trigger pulse is delivered into the spark gap switch, breakdown occurs at this moment. According to Figure 3.24, the distance need to be less than ~5.1 mm (extrapolation is used to calculate the maximum trigger pulse generator output voltage vs gap distance as in Figure 3.24) so that breakdown can happen. Figure 3.32 is the circuit of using DC power supplies and trigger pulse to induce a breakdown in the spark gap switch. Figure 3.33 is the test result. The black line is the square pulse from the function generator. The purple line is the VDP and the blue line is the VDP2. The spark gap is triggered as expected.

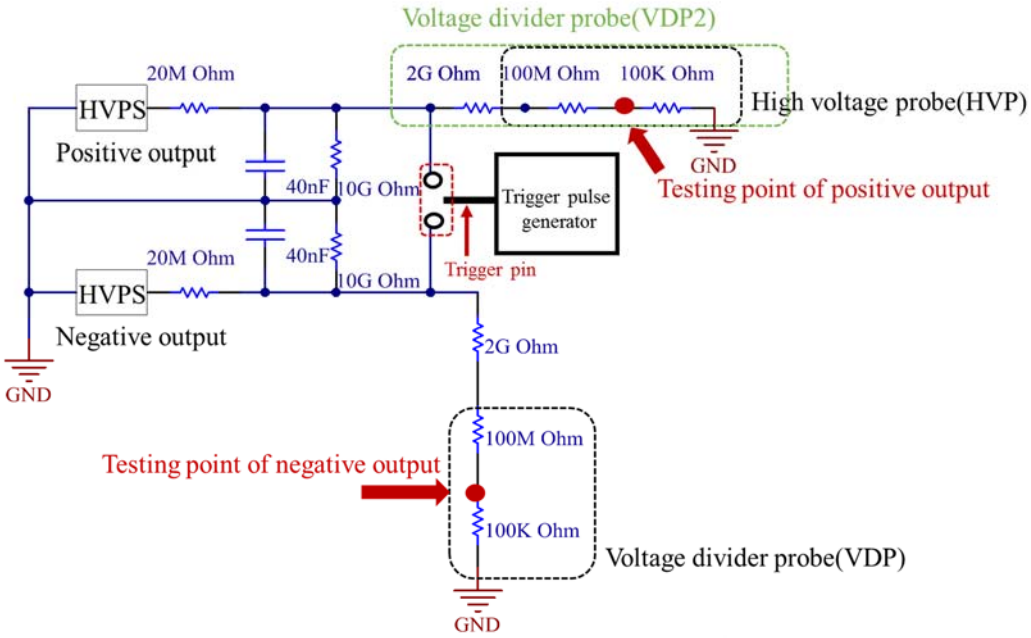

Figure 3.32 The circuit of using DC power supplies and trigger pulse to induce spark gap switch breakdown.

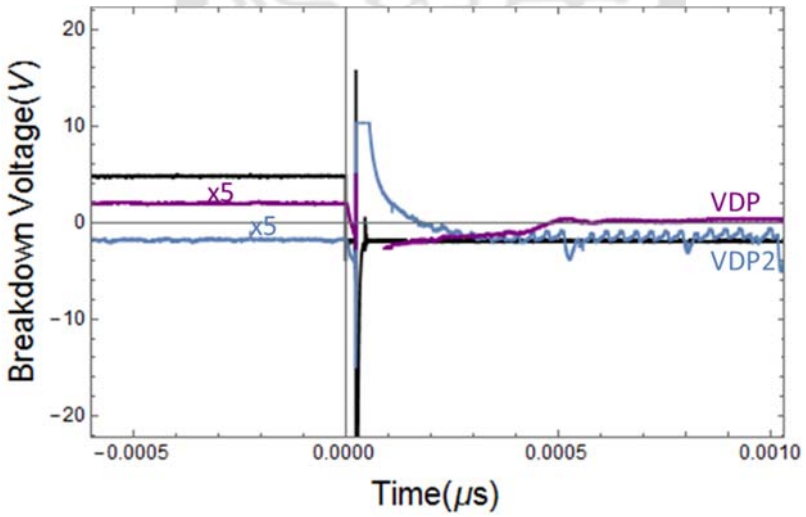

Figure 3.33 The test result of delivery the trigger pulse to the spark gap switch. The black line is the square pulse from the function generator. The purple line is the VDP and the blue line is the VDP2.

Chapter 4 RUST REMOVER RESULTS AND DISCUSSIONS

The rust remover using a small pulsed-power system was built and tested, and it is introduced in this chapter. Figure 4.1is the circuit of the pulsed-power system with rusted object. A current monitor (Pearson 301X) at point A is to measure the discharge current. The rusted object is connected to switch in series. Before the spark gap switch breakdowns, the voltage of the rusted object is the same as HVPS2. After the spark gap switch breakdown, the current will propagate through the rusted product.

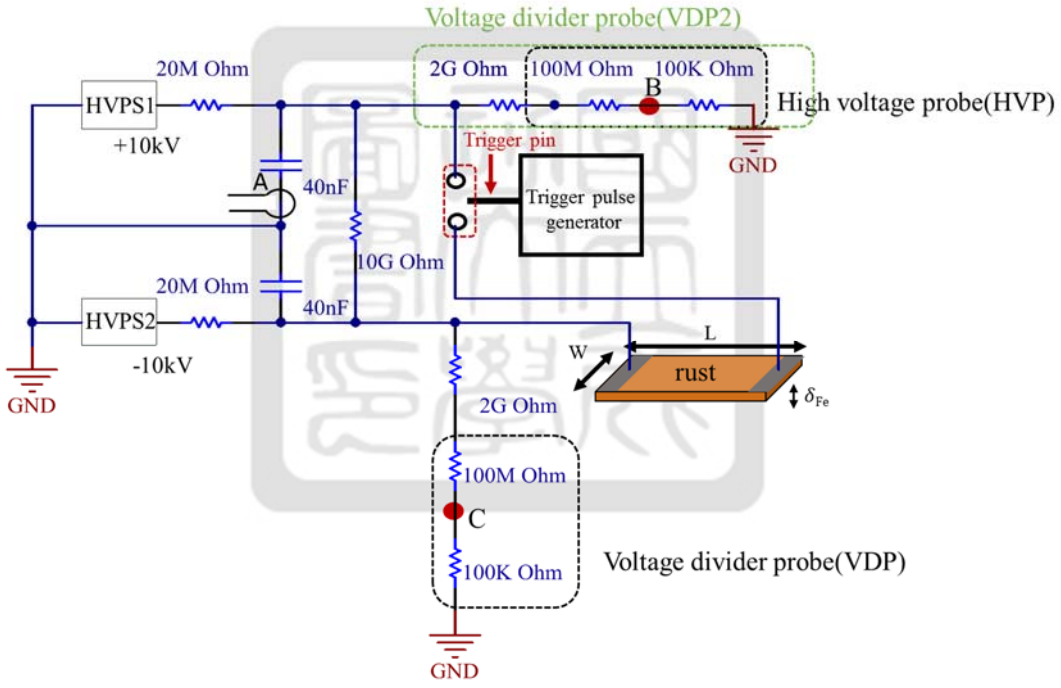

Figure 4.1 The circuit of the pulsed-power system with rusted object.

Figure 4.2 is the photo of the pulsed-power system. The whole system is placed in a 90 cm x 90 cm x 90 cm box made by using 15 mm thick acrylic. Edges of the acrylic box are connected to ground so that the current can be guided to ground and thus the energy can be released to ground when an arc to the sounding environment occurs. On the other hand,

capacitors may explode if the voltage across them exceed their working voltage. The acrylic box acts like a barrier for safety.

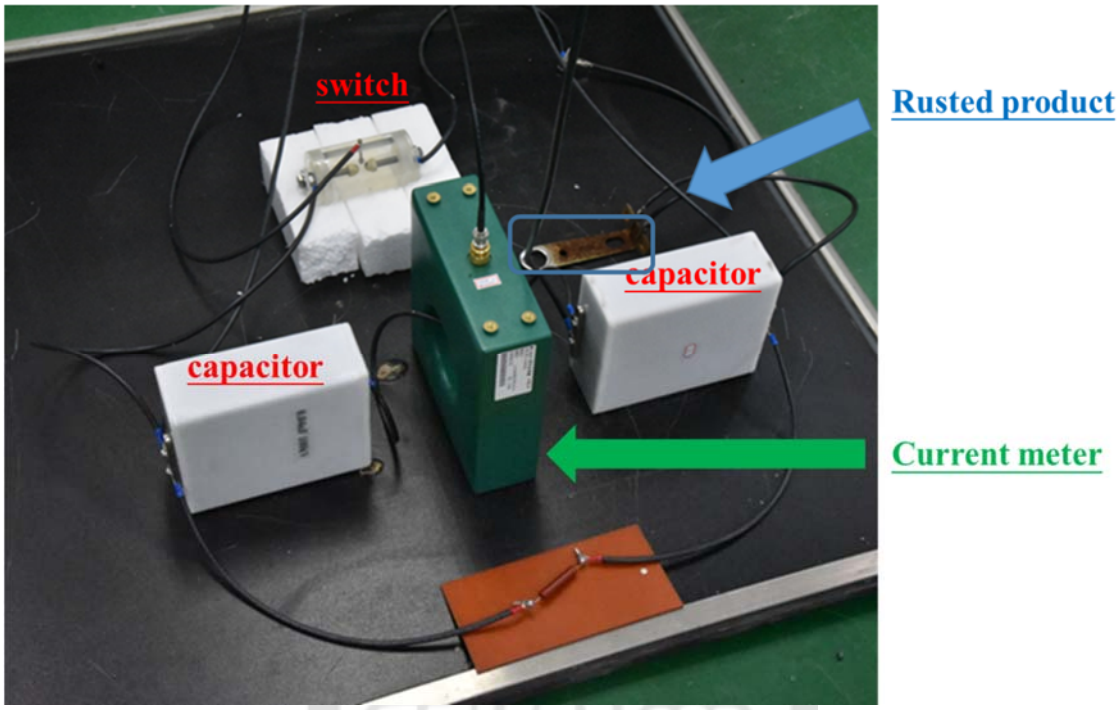

Figure 4.2 The device of pulsed power system of high voltage output and with current meter.

Figure 4.3 shows the rusted object before the current propagating through it. Figure 4.3 (a) and (b) are the front and the back side of the object, respectively. We used clips to connect the rusted object to the system. The red line and black line represent where clips locates. They are also shown in Figure 4.3 (c). The current will propagate through the rusted object between two clips.

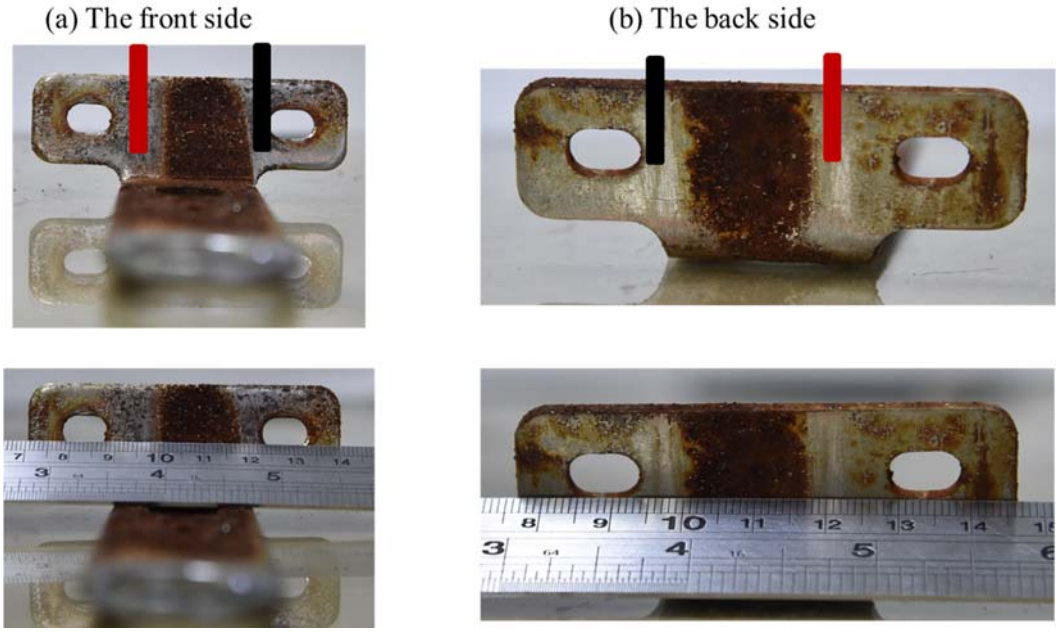

(c)

Figure 4.3 The rusted product before the current propagating the rusted product surface. (a) the front side (b) the back side. The red line and black line show the clip position like clips in (c).

The thickness of the rust on the rusted object is 0.5 mm while the skin depth of a current pulse is 0.4 μm. It would take more than 2500 shots to remove the rust. We tested with ~2880 shots. To implement the experiment that the function generator was set “Burst” model and one shot per 5 sec. Figure 4.4 is the rusted object after the current propagating through the rusted surface. The result didn’t meet our expectation. It didn’t remove the area of the 1.8

cm x 1.8 cm on the rusted surface. The most possible reason is that energy was released not only on the rusted surface but also on any (metal) surface along the current path. Nevertheless, the small spots in the red circles in Figure 4.5, where clips are located, are observed. The clean spots indicate that current did propagate through the object. In fact, it also indicates that to increase the resistance, i.e., to provide a localized ohmic heating, making the contact surface smaller can be an option since $R = \eta \frac{L}{A}$. Nevertheless, in the point of view of the pulsed-power system we plan to build in the future, we don't need to worry about the erosion of our cables.

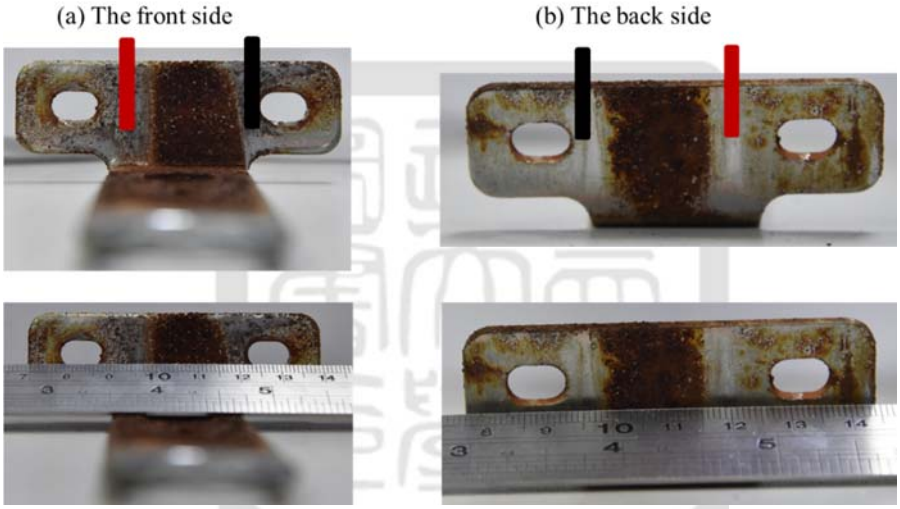

Figure 4.4 The rusted product after the current propagating the rusted product surface. (a) the front side (b) the back side.

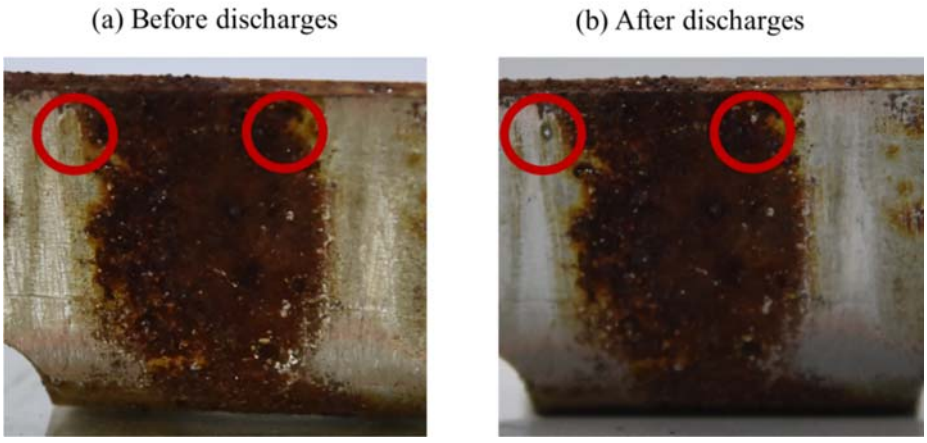

Figure 4.5 Compared before and after the current propagating the rusted product.

Even though the performance of the rust remover system is not as good as we expected, it still provides important information of our pulsed-power system. The key information is the inductance and the resistance of the whole system. Figure 4.6 is the current measurement during the process of removing rust. Black line (CH1) is a square, purple line (CH3) is the current which measured at point A in Figure 4.1. The system is activated ~ 18 μs after it is triggered (delay time). The voltage as well as the current oscillate during the discharge.

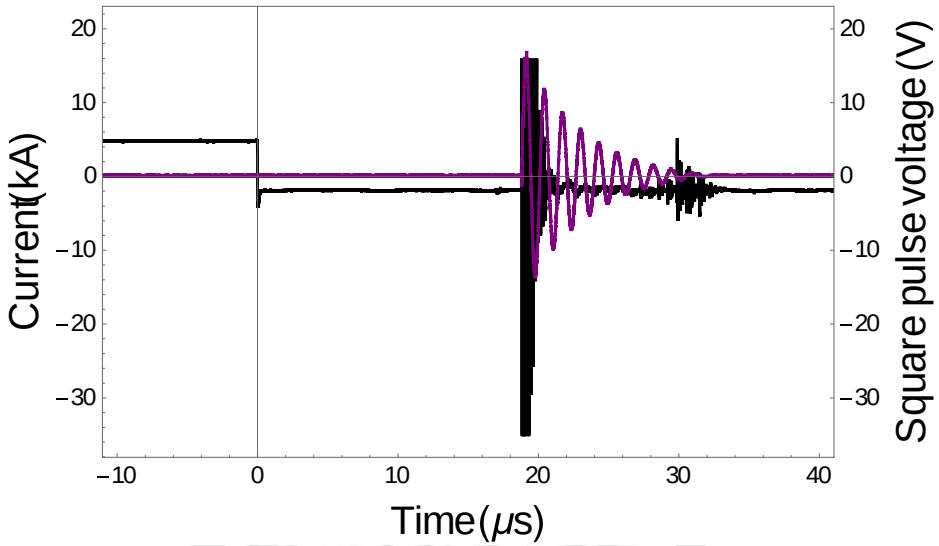

Figure 4.6 The data of the output current (purple) and the square pulse (black) by using pulsed-power system to remove the rust.

Figure 4.7 shows the current measurement on a smaller time scale at point A. It shows an under damped oscillation. It can be fitted with the under damped RLC circuit oscillation model given in section 2.1:

$$\mathrm{I(t)} = \frac{V_0}{\sqrt{\frac{L}{C} - \left(\frac{R}{2}\right)^2}} e^{-\frac{R}{2L}t} \sin\left(\sqrt{\frac{1}{LC} - \left(\frac{R}{2L}\right)^2}\, t\right) + I_{0ffset} \qquad (4.1)$$

where $\gamma = \frac{R}{2L}$ is the damping factor, $\omega = \sqrt{\frac{1}{LC} - \left(\frac{R}{2L}\right)^2}$ is the oscillation frequency and T_{offset} represents when the discharge starts.

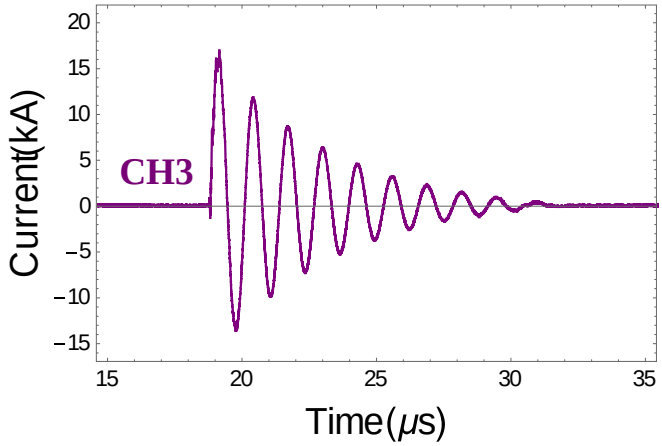

Figure 4.7 The current testing at the A point.

The inductance and resistance of our pulsed-power system can be calculated from the result of the curve fitting, i.e., L= $\frac{1}{C(\omega^2+\gamma^2)}$ and R= $\frac{2\gamma}{C(\omega^2+\gamma^2)}$. Notice that the capacitance C = 20 nF are used and L and R are inductance and resistance of the whole system. The curve fitting shows ω = (4.9 ± 0.1) x 10^6 sec^{-1} and thus L = 212 ± 85 nH. The impedance of the circuit is $\sqrt{L/C}$ = 3.3 Ω. Furthermore, the fitted result gives γ = 235,000 sec^{-1} and thus R = 1.00 ± 0.04 Ω. The oscillation frequency is (4.85 ± 0.1) x 106 sec^{-1} leading to a skin depth of 0.4 μm. We can calculate the power of our pulsed-power system which is about 230 kW for current fully damped on ~ 11μs.

On the other hands, there are some ideas of improvement the design of the rust remover. One idea is that we can decrease the distance of two clips which on the rusted object. When we decrease the area between two clips, the resistance will increase. According to the ohmic heating, when the energy release on the rusted object, the rust will get more energy than previous and melt rust as shown in Figure 4.8. The other idea is that we can set up the rusted object among two clips (electrodes) and the current passing through the rusted object frome one side to the other side directly as shown in Figure 4.9. This case can ensure the current passing through the rust and the energy release on it.

Figure 4.8 (a) previous case (b) improvement case. The orange line is the distance between two clips.

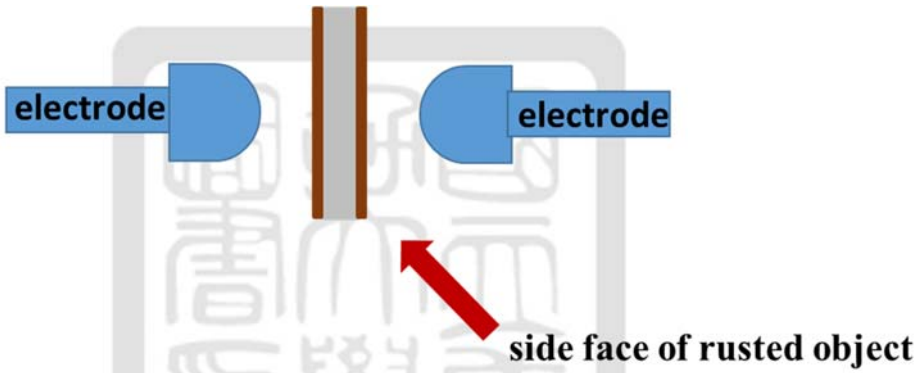

Figure 4.9 The improvement idea of the two clips position (electrodes). When the two electrodes breakdown, the current will passing through the rusted object from one side to the other side directly.

Chapter 5 SUMMARY

A rust remover using a small pulsed-power system was built and demonstrated. The principle of the rust remover is to use the skin depth effect due to the short pulse current provided by the pulsed-power system. To trigger the spark gap, we built a -18 kV output trigger pulse generator using an ignition coil for cars with 55 ± 0.4 μs rise time. The relationship between the distance of the gap and the breakdown voltage was tested.

In order to hold 18 kV, the distance need to be shorter than 5.1 cm so that a high voltage trigger pulse provided by our trigger pulse generator can induce breakdowns in the spark gap. The final design of the spark gap is 1.8 cm between two electrodes while the trigger pin is at the center place of two electrodes but 4.1 cm away from the axis of the spark gap. The total inductance and resistance of the pulsed-power system we built are 212 ± 85 nH, and 1 ± 0.04 Ω, respectively. The impedance is 3.3 Ω. The oscillation frequency is (4.85 ± 0.1) x 10^6 sec^{-1} leading to a skin depth of 0.4 μm. The averaged power of our pulsed-power system is about 230 kW before the output current is full damped in ~ 11 μs. After ~2880 shots, it's hardly to see any rust being cleaned as we expected. The most possible reason is that the energy was released not only on the rusted surface but also on any (metal) surface along the current path. However, it shows that we don't need to worry about the erosion on the cables in a pulsed-power system which will be built as the long term goal in our lab. There are two ideas of improving the design of the rust remover. One idea is to decrease the distance between two clips which on the rusted object. The other case is relocate the position of two clips (electrodes) so that current is for sure flowing through the rusted surface.

Reference

[1]Yifan Wu, “Repetitive and High Voltage Marx Generator Using Solid-state Devices”, IEEE Transactions on Dielectric and Electrical Insulation Vol. 14, No. 4; August 2007

[2] H. Bluhm,”Pulsed Power Systems Principles and Applications”, Springer, Germany, 2006

[3] Michael G. Mazarakis, “High current, 0.5-MA, fast, 100-ns, linear transformer driver experiments”, Phys. Rev. ST Aceel. Beams **12,** 050401(2009)

[4] A. A. Kim, “Development and tests of fast 1-MA linear transformer driver stages”, Phys. Rev. ST Aceel. Beams **12,** 050402(2009)

[5] J. R. Woodworth, “Low-inductance gas switches for linear transformer drivers”, Phys. Rev. ST Aceel. Beams **12,** 060401(2009)

[6] D. V. Rose, “Circuit models and three-dimensional electromagnetic simulations of a 1-MA linear transformer driver stage”, Phys. Rev. ST Aceel. Beams **13,** 090401(2010)

[7] E. Husain, “Analysis of Paschen curves for air, N_2 and SF_6 using the townsend breakdown equation”, IEEE. Transaction on Electrical Insulation, VOL. EI-17, NO. 4(1982)

[8] B. M. Kovalchuk, “Capacitor blocks for linear transformer driver stages”, Phys. Rev. Sci. Instrum. **85,** 013501(2014)

[9] M.G.Mazarakis, “A COMPACT, HIGH-VOLTAGE E-BEAM PULSER”, IEEE, 0-7803-5498-2, 6528415, (2002)

[10] https://en.wikipedia.org/wiki/Skin_effect

[11] http://tw.tek.com/high-voltage-probe-manual/p6015a

[12] http://uk.rs-online.com/web/p/fibre-optic-transceivers/8188855/

[13] https://en.wikipedia.org/wiki/Latch-up

[14] http://www.sandia.gov/z-machine/news/image_gallery.html

[15] http://web.tiscali.it/itischivasso/Progetti%20didattici/Area%20di%20Progetto.htm

[16]http://macao.communications.museum/eng/exhibition/secondfloor/MoreInfo/2_10_3_HowTransistorWorks.html

[17]https://zh.wikipedia.org/wiki/%E9%87%91%E5%B1%AC%E6%B0%A7%E5%8C%96%E7%89%A9%E5%8D%8A%E5%B0%8E%E9%AB%94%E5%A0%B4%E6%95%88%E9%9B%BB%E6%99%B6%E9%AB%94

[18] https://www.pcmag.com/encyclopedia/term/59900/igbt

[19] https://thinkelectronics.org/igbt/

[20] http://www.electronics-tutorials.ws/power/insulated-gate-bipolar-transistor.html

[21] http://www.altium.com/

國立成功大學

Appendix

Pulsed power laboratory safety guidelines from Texas Tech University

General Electrical

1. Be well aware of the hazards that exist with the standard 120VAC power. This is potentially more dangerous than any other power source in the laboratory due to its commonplace use and high-current capabilities. The main breaker panels are capable of delivering in excess of 200 amps per phase.

2. Familiarize yourself with the location of the main breaker panels and auxiliary panels and the general areas which they service. Keep panel areas and access to them free of clutter.

3 Make positive connections to your power outlets. Do not use faulty plugs, cords, connectors, or receptacles. Have them replaced or repaired immediately.

4. When repairing or assembling a power cord or extension, learn and use the proper wiring code to insure correct polarity. For most cases in this lab, our extension cord cable is black, three conductor cable, 16/3, one black, one white, one green. Most commercially available plugs, connectors, and receptacles are color coded. Make connections as follows:

   Black (or hot) to brass screw.
   White (or neutral) to silver screw.
   Green (or ground) to green screw.

   Some cables may not be color coded in this same manner but remember, you still have hot, neutral, and ground.

5 Never work on a live circuit or tap into live wires. Locate the switch, fuse, or circuit breaker and disconnect the power before starting to work on the circuit. Label this service so others will know not to reconnect while work is in progress.

6. Do not replace a fuse or reset a circuit breaker on a "blown" circuit until the cause of the trouble has been found and corrected.

High Voltage

Consider any voltage level greater than our nominal 120VAC/3P phase as being "High Voltage".

2. Never work alone when using "High Voltage". You must have at least one other person present during a "High Voltage" experiment.

3. The experimenter shall provide some warning that the "High Voltage" is `on'. This can best be done by means of a flashing red light and a "Danger High Voltage" warning sign. Also extend a verbal warning to those persons working on other projects in close proximity: "Charging", "High Voltage".

4. Confine all "High Voltage" experiments to controlled access areas. Depending on size, this can be done by placing the experiment within a grounded screen room or metal box or by blocking off the area by a rope barricade. Be aware of other persons close-by, and be well aware of "passers-by". Be sure that you yourself do not disregard someone else's barricades.

5. Designate some point of your experiment as "experimental ground". Reference all equipment grounds to this point. Then connect with one 6 AWG cable, or larger, that point to the grounding grid or to building ground.

6. Provide some method of discharging "High Voltage" points of your experiment to insure safe approach and handling. This can be automatic or manual, by means of a "high voltage" relay or by "shorting sticks". The discharge should be back to "experimental ground" through some resistance. In case of a capacitor being used with no reference to ground, the discharge must be between the capacitor terminals. This short circuit should remain in place when the experiment requires maintenance or is not in operation.

7 Before handling energy discharge/storage capacitors, make sure they are discharged by means of "resistive shorting sticks", then insure that they do not acquire a static charge by attaching "direct shorting sticks". Finally, attach a metal strap or wire between the terminals.

8 Never view a high energy discharge with the naked eye. Make use of filters and remote monitor.

9 Use protective shields to insure safety in case of catastrophic apparatus or component failure. Do not take for granted that your designs and assemblies are without fault or defect. Watch for signs of material fatigue.

10. Protect your ears. Hearing protectors are available, so make use of them. An open-air discharge of most experiments in this lab are of high enough energy to cause hearing loss.

The derivation of the RLC circuit

Initial conditions: the voltage of the capacitor at t = 0 is V (t = 0) = V_0 , I (t = 0) = 0.

$$V - IR - L\frac{dI}{dt} = 0 \tag{1}$$

with current

$$\mathrm{I} = \frac{dQ}{dt} = -C\frac{dV}{dt} \tag{2}$$

$$\mathrm{V} + \mathrm{RC}\frac{dV}{dt} + LC\frac{d^2V}{dt^2} = 0 \tag{3}$$

$$\frac{d^2V}{dt^2} + \frac{R}{L}\frac{dV}{dt} + \frac{1}{LC}V = 0 \tag{4}$$

Let $V = e^{Dt}$ and substitute it into equation (4):

$$D^2 + \frac{R}{L}D + \frac{1}{LC} = 0 \tag{5}$$

The solution of D is

$$\frac{-\frac{R}{L} \pm \sqrt{\left(\frac{R}{L}\right)^2 - \frac{4}{LC}}}{2}$$

$$= -\frac{R}{2L} \pm \sqrt{\left(\frac{R}{2L}\right)^2 - \frac{1}{LC}} \tag{6}$$

and V is

$$e^{-\frac{R}{2L}t}\left(\alpha' e^{\sqrt{\left(\frac{R}{2L}\right)^2 - \frac{1}{LC}}\,t} + \beta' e^{\sqrt{\left(\frac{R}{2L}\right)^2 - \frac{1}{LC}}\,t}\right)$$

$$\equiv e^{-\gamma t}\left(\alpha' e^{\sqrt{\left(\frac{R}{2L}\right)^2 - \frac{1}{LC}}\,t} + \beta' e^{\sqrt{\left(\frac{R}{2L}\right)^2 - \frac{1}{LC}}\,t}\right) \tag{7}$$

Where $\gamma \equiv \frac{R}{2L}$.

(a) Under-damped condition where $\left(\frac{R}{2L}\right)^2 - \frac{1}{LC} < 0$:

Equation (7) can be rewritten as

$$\begin{aligned} \mathrm{V} &= e^{-\gamma t}\left(\alpha' e^{i\sqrt{\frac{1}{LC}-\left(\frac{R}{2L}\right)^2}\,t} + \beta' e^{i\sqrt{\frac{1}{LC}-\left(\frac{R}{2L}\right)^2}\,t}\right) \\ &= e^{-\gamma t}\left(\alpha' e^{i\omega t} + \beta' e^{-i\omega t}\right) \\ &\equiv e^{-\gamma t}[\alpha\, cos(\omega t) + \beta\, sin(\omega t)] \end{aligned} \tag{8}$$

where $\omega \equiv \sqrt{\frac{1}{LC} - \left(\frac{R}{2L}\right)^2}$. Substitute the initial condition V(t=0)=V_0 into equation (8):

$$\begin{aligned} \mathrm{V(t=0) = V_0} \quad &= e^{-\gamma 0}[\alpha\, cos(\omega 0) + \beta\, sin(\omega 0)] = \alpha \\ \mathrm{V} \quad &= e^{-\gamma t}[V_0\, cos(\omega t) + \beta\, sin(\omega t)] = \alpha \end{aligned} \tag{9}$$

$$\begin{aligned} \mathrm{I} \quad &= -\mathrm{C}\frac{dV}{dt} = -\mathrm{C}\frac{d}{dt}\left[e^{-\gamma t}\left(V_0\, cos(\omega t) + \beta\, sin(\omega t)\right)\right] \\ &= -\mathrm{C}\Big[-\gamma e^{-\gamma t}\left(V_0\, cos(\omega t) + \beta\, sin(\omega t)\right. \\ &\qquad \left. + e^{-\gamma t}\left(-\omega V_0 sin(\omega t) + \omega\beta cos(\omega t)\right)\right)\Big] \\ &= -\mathrm{C}e^{-\gamma t}\Big[-\gamma\left(V_0\, cos(\omega t) + \beta\, sin(\omega t)\right. \\ &\qquad \left. + e^{-\gamma t}\left(-\omega V_0 sin(\omega t) + \omega\beta cos(\omega t)\right)\right)\Big] \end{aligned} \tag{10}$$

Apply the initial condition I(t=0)=0

$$\mathrm{I(t=0) = 0} \quad = -\mathrm{C}[-\gamma V_0 + \omega\beta] \;\rightarrow\; \beta = \gamma\frac{V_0}{\omega}$$

$$\begin{aligned} \mathrm{V} \quad &= e^{-\gamma t}\left[V_0\, cos(\omega t) + V_0\frac{\gamma}{\omega}\, sin(\omega t)\right] \\ &= V_0 e^{-\gamma t}\left[cos(\omega t) + \frac{\frac{R}{2L}}{\sqrt{\frac{1}{LC} - \left(\frac{R}{2L}\right)^2}}\, sin(\omega t)\right] \end{aligned} \tag{11}$$

$$\mathrm{I} = -\mathrm{C}e^{-\gamma t}\left[-\gamma\left(V_0 cos(\omega t) + \beta sin(\omega t) + \left(-\omega V_0 sin(\omega t) + \omega\beta cos(\omega t)\right)\right)\right]$$

$$= \mathrm{C}e^{-\gamma t}\left[\left(-\gamma V_0 + \omega\frac{\gamma V_0}{\omega}\right)cos(\omega t) + \left(\gamma\gamma\frac{\gamma V_0}{\omega} + \omega V_0\right)sin(\omega t)\right]$$

$$= V_0 C e^{-\gamma t}\left(\frac{\gamma^2}{\omega} + \omega\right)sin(\omega t) = V_0 C e^{-\gamma t}\left(\frac{\gamma^2 + \omega^2}{\omega}\right)sin(\omega t)$$

$$= V_0 C e^{-\gamma t}\frac{\left(\frac{R}{2L}\right)^2 + \frac{1}{LC} - \left(\frac{R}{2L}\right)^2}{\sqrt{\frac{1}{LC} - \left(\frac{R}{2L}\right)^2}}sin(\omega t)$$

$$= \frac{V_0}{L}\frac{1}{\sqrt{\frac{1}{LC} - \left(\frac{R}{2L}\right)^2}}e^{-\gamma t}sin(\omega t)$$

$$= \frac{V_0}{\sqrt{\frac{L}{C} - \left(\frac{R}{2}\right)^2}}e^{-\frac{R}{2L}t}sin\left(\sqrt{\frac{1}{LC} - \left(\frac{R}{2L}\right)^2}\,t\right) \quad (12)$$

(b) Critical-damped condition where $\left(\frac{R}{2L}\right)^2 - \frac{1}{LC} = 0$:

D in equation (6) becomes

$$\mathrm{D} = -\frac{R}{2L} \quad (13)$$

$$\mathrm{V} = (\alpha + \beta t)e^{-\frac{R}{2L}t} \equiv (\alpha + \beta t)e^{-\gamma t} \quad (14)$$

Where $\gamma \equiv \frac{R}{2L}, i.e., \frac{1}{LC} = \gamma^2$. Apply the initial condition V(t=0) = V_0:

$$\mathrm{V(t=0) = V_0} \quad = (\alpha + \beta 0)e^{-\gamma 0} = \alpha$$

$$\mathrm{V} \quad = (V_0 + \beta t)e^{-\gamma t} \quad (15)$$

$$\mathrm{I} \quad = \left(-\mathrm{C}\frac{\mathrm{dV}}{\mathrm{dt}} = -\mathrm{C}[\beta e^{-\gamma t} - \gamma(V_0 + \beta t)e^{-\gamma t}]\right)$$

$$= -\mathrm{C}e^{-\gamma t}[\beta - \gamma(V_0 + \beta t)]. \quad (16)$$

Apply the initial condition I(t=0)=0:

$$\text{I(t=0) = 0} \quad = -Ce^{-\gamma 0}[\beta - \gamma(V_0 + \beta 0)] \rightarrow \beta = \gamma V_0$$

$$\text{V} \quad = (V_0 + \gamma V_0 t)e^{-\gamma t} = V_0(1+\gamma t)e^{-\gamma t}$$

$$= V_0\left(\left(1 + \frac{R}{2L}t\right)e^{-\frac{R}{2L}t}\right) \tag{17}$$

$$\text{I} \quad = -\text{C}\frac{dV}{dt} = -\text{C}\frac{d}{dt}[V_0(1+\gamma t)e^{-\gamma t}]$$

$$= -V_0 C[\gamma e^{-\gamma t} + (1+\gamma t)(-\gamma)e^{-\gamma t}]$$

$$= -V_0 C e^{-\gamma t}(\gamma - \gamma - \gamma^2 t)$$

$$= V_0 C \gamma^2 t e^{-\gamma t} = V_0 C \frac{1}{LC} t e^{-\gamma t}$$

$$= \frac{V_0}{L} t e^{-\frac{R}{2L}t} \tag{18}$$

(c) Over-damped condition where $\left(\frac{R}{2L}\right)^2 - \frac{1}{LC} > 0$:

Let $\sum \equiv \sqrt{\left(\frac{\text{R}}{2\text{L}}\right)^2 - \frac{1}{\text{LC}}}$ and $\gamma \equiv \frac{\text{R}}{2\text{L}}$ then

$$\text{V} = e^{-\gamma t}\left(\alpha e^{\sum t} + \beta e^{\sum t}\right) \tag{19}$$

Apply the initial condition V(t=0)= V_0

$$\text{V(t=0) = V}_0 \quad = e^{-\gamma 0}\left(\alpha e^{\sum 0} + \beta e^{\sum 0}\right) = \alpha + \beta \tag{20}$$

$$\text{I} \quad = -\text{C}\frac{dV}{dt} = -\text{C}\frac{d}{dt}\left[e^{-\gamma t}\left(\alpha e^{\sum t} + \beta e^{\sum t}\right)\right]$$

$$= -\text{C}\left[-\gamma e^{-\gamma t}\left(\alpha e^{\sum t} + \beta e^{\sum t}\right) + e^{-\gamma t}\left(\sum \alpha e^{\sum t} - \sum \beta e^{\sum t}\right)\right]$$

$$= -\text{C}e^{-\gamma t}\left[-\gamma\left(\alpha e^{\sum t} + \beta e^{\sum t}\right) + \left(\sum \alpha e^{\sum t} - \sum \beta e^{\sum t}\right)\right]$$

$$= -\text{C}e^{-\gamma t}\left[\alpha\left(\sum -\gamma\right)e^{\sum t} + \beta\left(\sum +\gamma\right)e^{-\sum t}\right]$$

(21)

Apply the initial condition I(t=0)=0:

$$\text{I(t=0)=0} = -\text{C}[\alpha(\sum -\gamma) - \beta(\sum +\gamma)] = 0$$

$$\alpha(\sum -\gamma) = \beta(\sum +\gamma). \tag{22}$$

From equation (21)

$$\beta = \frac{\sum -\gamma}{\sum +\gamma}\alpha \tag{23}$$

Substitute equation (22) into equation (20)

$$\alpha\left(1+\frac{\sum-\gamma}{\sum+\gamma}\right)=\alpha\frac{\sum+\gamma+\sum-\gamma}{\sum+\gamma}=\alpha\frac{2\sum}{\sum+\gamma}=V_0 \tag{24}$$

$$\alpha=\frac{\sum+\gamma}{2\sum}V_0 \tag{25}$$

$$\beta=\frac{\sum-\gamma}{2\sum}V_0 \tag{26}$$

$$V=e^{-\gamma t}\left(\frac{\sum+\gamma}{2\sum}V_0e^{\sum t}+\frac{\sum-\gamma}{2\sum}V_0e^{-\sum t}\right)$$

$$=\frac{V_0}{2\sum}e^{-\gamma t}\left[\left(\sum+\gamma\right)e^{\sum t}+\left(\sum-\gamma\right)e^{-\sum t}\right] \tag{27}$$

$$I=-Ce^{-\gamma t}\left[\alpha\left(\sum-\gamma\right)e^{\sum t}-\beta\left(\sum+\gamma\right)e^{-\sum t}\right]$$

$$=-Ce^{-\gamma t}\left[\frac{\sum+\gamma}{2\sum}V_0\left(\sum-\gamma\right)e^{\sum t}-\frac{\sum-\gamma}{2\sum}V_0\left(\sum+\gamma\right)e^{-\sum t}\right]$$

$$=-\frac{CV_0}{\sum}\left(\sum{}^2-\gamma^2\right)e^{-\gamma t}\left(\frac{e^{\sum t}-e^{\sum t}}{2}\right)$$

$$=-\frac{CV_0}{\sum}\left(\sum{}^2-\gamma^2\right)e^{-\gamma t}sinh\left(\sum t\right) \tag{28}$$

Note that

$$\sum{}^2-\gamma^2=\left(\frac{R}{2L}\right)^2-\frac{1}{LC}-\left(\frac{R}{2L}\right)^2=-\frac{1}{LC} \tag{29}$$

$$I=\frac{V_0/L}{\sqrt{\left(\frac{R}{2L}\right)^2-\frac{1}{LC}}}e^{-\gamma t}\sinh(\sum t)$$

$$=\frac{V_0}{\sqrt{\left(\frac{R}{2}\right)^2-\frac{L}{C}}}e^{-\frac{R}{2L}t}\sinh\left(\sqrt{\frac{1}{LC}-\left(\frac{R}{2L}\right)^2}\,t\right) \tag{30}$$